Sizing up community structure:

Exploring latitudinal gradients in Northeastern Pacific Patellogastropoda (Mollusca, Gastropoda) body size with high-throughput morphometric imaging

Sara S. Kahanamoku-Snelling

Pincelli Hull, Advisor

Derek Briggs, Second Reader

Seth Finnegan and David Lindberg, Secondary Advisors

5 May 2016

A Senior Thesis presented to the faculty of the Department of Geology and Geophysics, Yale University, in partial fulfillment of the Bachelor's Degree.

Abstract

Individual body size can vary widely between different communities, many of which are spatially adjacent. This variation is particularly important to ecologists as the size structure of these communities is closely tied to their ecology (i.e. their dynamics and energetics) as well as to individual life and evolutionary histories. Although ecologists commonly refer to Bergmann's rule (an increase in body size with latitude), community body size is rarely directly measured in marine invertebrates due to the difficulty of obtaining body size data for entire assemblages. Here we examine individual variation in an understudied group, Patellogastropoda (true limpets), across a latitudinal gradient (namely, the Northeastern Pacific). The transect studied, which ranges from Alaska to Baja, California, showcases large amounts of environmental variation and encompasses a number of environmental and faunal provinces. Thanks to recent advancements in the speed and quality of morphological measurements, collection of large, individual-level datasets is no longer infeasible. However, it has previously only been possible for microorganisms. In light of this, we apply a novel method, macroscopic high-throughput imaging, that allows for automated collection of morphological data for entire assemblages, to the Northeastern Pacific Patellogastropoda. Previous studies of this system for a similar group (Bivalvia) which utilized exemplar measurements found that size structure was invariant across the transect. Using individual-level, community data, we find that size structure does vary along the transect, and that body size increases with latitude, confirming Bergmann's rule for Patellogastropoda. However, we find that the resolution at which data is collected influences the results obtained from the data, as intraspecific trends do not match broad inter-specific trends in size. In addition, the scale at which measurements are taken (i.e. whether they are empirical versus exemplar) greatly alters the distributions obtained. We also find that the greatest predictors of body size variation are biotic correlates (i.e. community structure and species present), rather than environmental variables. As such, Patellogastropod community body size varies only weakly with latitude and environment, but is closely related to community composition. This finding sheds light on the importance of interspecific interactions, which are especially strong in Patellogastropod communities, as a determinant of faunal body size trends.

Contents

Background

Introduction

Community body size has long been observed to vary systematically with latitude. This pattern, also known as Bergmann's rule, has intrigued biologists and been a constant subject of debate for the past 150 years. Bergmann's rule, which was coined prior to the *Origin of Species* in the mid-nineteenth century, posits that body size increases with latitude (Bergmann 1848, in Berke et al. 2013). This rule has shown to hold true for cases in many groups, such as mammals (Ashton et al. 2000), amphibians (Ashton 2002), insects (Kaspari and Vargo 1995), and a number of marine invertebrates (reviewed in Partridge and Coyne 1997; Daufresne et al. 2009, Sommer et al. 2016). However, the tendency for body size to increase with latitude is not seen in all cases within these groups, and debate continues about whether the rule is generalizable (e.g. Berke et al. 2013).

The importance of deconstructing body size trends in communities that span large swaths of space is reflected in the continuing controversy surrounding Bergmann's rule. This rule has been so intensively studied, and for so long, because community body size influences and is influenced by individual-level metabolism as well as community-level dynamics. Body size is determined in part by metabolism, which shapes an individual's development, age at maturity, and life span (Brown et al. 2004), as well as its physiology (LaBarbera 1986), reproduction (Blueweiss et al. 1978), and even its evolutionary direction (Jablonski 1996). Additionally, body size may be influenced by a group's evolutionary history (Cope's rule; Heim et al. 2015) as well as its environment (Blackburn et al. 1999, Berke et al. 2013). Body size not only determines the fate of individual organisms; it also influences community-level traits. The interaction of multiple individuals in a community results in differing rates of competition, predation, and carrying capacity, as well as species diversity, and

these communities can interact to determine ecosystem processes like overall biomass production (Brown et al. 2004). That is, these individual interactions, which are influenced by body size, help to determine overall body size structure. In addition, community dynamics, or how the structure and composition of communities change through time, is largely influenced by body size, particularly because size determines the success rate of individuals, which in turn dictates species' success. It is well known that community structure is highly variable, and that given each species' unique distribution and abundance, as well as large environmental variation through space, no two communities are exactly alike (Brown 1995). However, what is unclear whether it is species' interactions in these communities or environmental influence that determines community size structure.

Hence, the uncertainty that continues with regard to the validity of Bergmann's rule centers around its fundamental claim that *environment* is the largest determinant of body size. While it is true that some organisms increase in size with a cooling environment (Partridge and Coyne 1997), and vice-versa (Daufresne et al. 2009), not every organism follows this trend. In direct contrast to the posited size-latitude relationship, many groups achieve opposite-Bergmann clines or U-shaped distributions along their respective latitudinal gradients (reviewed in Berke et al. 2013). These antithetical trends have caused a number of biologists to conclude that broadly generalizable macroecological patterns do not exist for groups like marine invertebrates (Roy et al. 2000, 2001; Berke et al. 2013), which are large, cosmopolitan, and widely diverse.

However, it is likely that the coarse scale at which body size is measured contributes to a muddled understanding of the rule. It is not agreed upon at what level Bergmann's rule should be applied: some believe that it should be appropriate on a broader phylogenetic scope, whereas others feel that it is best examined intraspecifically (Meiri 2011). The majority of studies tend to be applied at the former resolution, choosing phylogenetic generality over assemblage-level specificity. While more specific studies are slowly becoming common, those that have been done rarely examine trends at the species level, and if they do, they rely on species averages (i.e. exemplar measurements such as maximum or mean size, applied for an entire species) rather than on empirical, individual body size measurements. These exemplar measurements ignore intraspecific variation, and thus smooth over the individual-level processes that influence community body size. While some believe that this individual variation is wrapped up in community size structure, and thus is not necessary to

measure, it is clear that overly general studies of size produce indeterminate or contradictory trends (e.g. Roy et al. 2000, Berke et al. 2013). As such, it has been proposed that a full understanding of macroecological patterns would require global datasets on body size (Berke et al. 2013), which should take individual variation into account and span across large, environmentally variable regions of space.

Body size and mollusks

Marine invertebrates are particularly abundant in the fossil record, making them the most common (and often only) biotic record of the history of life. Studies of marine invertebrates often focus on community body size, as one might expect given the dual importance of these organisms and size as a metabolic and evolutionary proxy. Mollusca is a particularly well-documented group, as mollusks have dominated marine ecosystems since nearly the beginning of the Phanerozoic (Payne et al. 2014). However, most studies of molluscan body size are limited, as they necessarily use species exemplars due to the difficulty of collecting individual-level data for such a broad group. In addition, while past examinations of body size trends in molluscans attempt to capture as much environmental, ecological, and phylogenetic variability as is possible, they are often (and necessarily) reductive, and focus their investigations on a few key variables, such as species average size and size frequency (as a proxy for community structure) or latitude (as a proxy for environment; e.g. Roy et al. 2001). Though these measurements are easily obtained, they are not necessarily the best descriptors of actual trends, as they do not reflect organismal or spatial variability.

In addition, studies tend to center on a few large molluscan groups, such as bivalves, brachiopods, or gastropods, and ignore smaller groups even though they, too, are widespread. One such underutilized molluscan group is the Patellogastropoda, or the true limpets. These rocky intertidal organisms live in highly variable environments, and are cosmopolitan—they can be found along nearly every coastline in the world, and have probably been clinging to those rocks for millennia. In addition, the size of this group—patellogastropods are composed of just 8 families, which are geographically segregated (Lindberg 2015 pers. com.)—means that a small number of species interact in a given space. Though they are not alone in their occupation of the shoreline, patellogastropods have evolved to be highly tolerant of constant exposure to air, heat, and wave

forces, and are nearly alone in their inhabitation of this extreme, small world. Though they are sometimes the victims of predation, their predators are few and far between. As such, they are more highly subject to strong community interactions, as their rough living situation necessitates greater territorialism (Fenberg 2011) and competition (Haven 1973). Given that this group is phylogenetically limited and experiences a confluence of environmental and biotic pressures, it presents a unique opportunity for re-examination of individual-level community trends in variable environments. Patellogastropods may be small, both in stature as well as in terms of species richness, but they offer a perfect study system in which to examine whether environment or community structure is a larger determinant of body size.

Latitudinal gradients and the intertidal zone: a world of variability

The variability of latitudinal gradients across large regions of space is enhanced by conditions in the intertidal zone, which can change dramatically across spaces on the order of meters. The intertidal (also known as the littoral zone) is underwater at high tide and and above water at low tide, thus subjecting its inhabitants (including patellogastropods) to varying degrees of dessication, extreme temperature change, and the mechanical forces of incoming waves and changing tides. Because the intertidal itself is highly variable, it contains a number of different niches, or ecosystems, at once. Those that reside in the high intertidal niche rarely, if ever, are fully submerged, making them the least marine of all; the mid-range inhabitants have a foot (digitate or not) in both the marine and the terrestrial realm, and those that live in the lowest intertidal only occasionally find that their usual medium has receded and left them exposed. As such, intertidal species are subject to extremely variable environmental conditions, and their life histories should reflect this dynamism accordingly. Add a latitudinal gradient into the equation, and this multi-dimensional space encapsulates a world's worth of information.

The northeastern Pacific Basin, or the western edge of the North American continent, is a particularly popular study area, as it contains a strong latitudinal gradient in temperature and productivity. Latitudinal gradients are useful for understanding species-environment interactions through space, which can then be applied to studies of species-environment interactions through time. This particular latitudinal gradient is highly sampled and studied, likely as a result of its

accessibility. Investigations of size trends in molluscans commonly include the Northeastern Pacific (e.g. Roy et al. 2000, Roy and Martien 2001, Roy et al. 2001, Roy et al. 2002, Berke et al. 2013). However, due to the difficulty of sampling along a 5000 km transect, these size studies tend to simplify their data collection by using species presence-absence data and exemplar measurements of size (i.e. species averages). No individual-level studies of size have been previously undertaken for this transect.

One such study, Roy et al. (2000), collected size data from Alaska to Baja, California, along the edge of the Eastern Pacific Basin. This study used species averages (namely, the geometric mean of length and height for the largest known specimen of each species) to obtain measurements of size, and applied these averages using presence-absence data for 914 species of bivalves in 5 faunal zones (Arctic, Oregonian, Californian, Transition, and Panamic). They found invariant size-frequency distributions across these zones, thus concluding that size structure does not change along the transect, and that size trends such as Bergmann's rule do not apply for Northeastern Pacific bivalves. While the methods in this study were necessarily reductive given the limitations of studying populations at the time, they may influence the conclusions drawn from the data. It is likely that exemplar measurements (especially measurements that use maximum size as representative) do not reflect community-level size structure, and that the size-frequency distributions generated by Roy et al. are at too coarse of a resolution to depict accurately the size trends present for the group studied. As such, a reinvestigation into community-level molluscan size structure in the Northeastern Pacific is necessary for definitive understanding of size trends (e.g. Bermann's rule) in the modern, which can then be translated for paleoecological use.

Motivation for study

New advances in rapid morphometrics allow population-level study that approximates natural size distributions. High-throughput imaging dramatically reduces processing time and allows for study of a greater volume of individuals than was previously possible using traditional morphometrics. In addition, advances in morphometric software increase the types and number of measurements that can be obtained from these individuals. However, high-throughput morphometric imaging has previously only been utilized for microfossils, e.g. planktonic foraminifera (Hull et al., in prep). It

has been established that a large amount of data is necessary to study community-level size trends in the Northeastern Pacific. Given that high-throughput morphometric software has already been developed, a size study requiring large numbers of individuals is the perfect test of the applicability of the method for macroecological study of groups other than foraminifera.

This study aims to be the first test of the applicabilty of Hull et al.'s morphometric software suite to macroscopic organisms. This software has the potential to make morphometric study of macroscopic body fossils much more efficient, and its widespread use would allow an increase in the number of population-level paleontological datasets available. In this study, we investigate community-level size trends of Northeastern Pacific Patellogatropoda (Mollusca, Gastropoda) using the collections housed at the University of California Museum of Paleontology (UCMP). Because these collections were largely uncatalogued, they required rapid digitization to fulfill museum efforts to digitize specimens for electronic study (i.e. via iDigBio and the Paleobiology Database). In addition, given the close relation of Patellogastropoda (limpets) to bivalves, the group studied in Roy et al. (2000), they are a good focus group for re-evaluation of size trends found in the Eastern Pacific.[1]

Questions and expectations

This study addresses four central questions. First, we investigate the patterns in limpet community body size from Alaska to Baja, and attempt to uncover how these patterns vary within and among species. Second, we examine whether these patterns are scale-dependent—that is, does that latitudinal bin size examined affect what trends are apparent?—or whether the patterns we observe are due to sampling bias. Third, we investigate patterns of environmental change along the study transect, particularly in relation to biogeographic provinces. Finally, we attempt to explain, in part, the drivers of limpet community body size distributions. Are these distributions determined most strongly by environment, or do biotic effects (i.e. the presence and absence of species, as well as intraspecific interactions) play the largest role in determining community body size? In particular, we aim to understand the community-level patterns and determinants of size.

---

[1]For further information on Patellogastropod biology and taxonomy, refer to the Appendix (page 54.)

Methods

Sampling

Samples of modern Patellogastropoda from the University of California Museum of Paleontology (UCMP) collection at the University of California, Berkeley were imaged. Sample collections were grouped by locality, and all sample lots from localities in the Northeastern Pacific, from the subtropics (Southernmost Baja California, latitude $\sim 22°$ N) to the Arctic (Northern Alaska, latitude $\sim 60°$ N), were withdrawn. Lots were typically organized by location and type, such that each lot represented a single species collected at a single site. A majority of sample identification tags were updated to reflect modern Patellogastropod taxonomy. Lot sizes ranged from a single specimen to >300 individuals (e.g. Figure 2, page 18). All Northeastern Pacific lots within the specified latitudinal transect were imaged irrespective of curation status, such that a majority of the samples were previously not assigned UCMP specimen numbers or were not searchable on the UCMP online database (ucmpdb.berkeley.edu). Preliminary curation during imaging resulted in the assignment of specimen lot numbers to each group of individuals that were uncatalogued prior to imaging (UCMP numbers 130000 through 130794) as well as in the digitization of previously unavailable specimen information.

Sites from which specimens were collected were coded as UCMP locality numbers (e.g. D8919) and locality strings (e.g. "Monterey, CA"). Locality strings were matched to latitude and longitude coordinates using GEOLocate (http://www.museum.tulane.edu/geolocate/). Uncertainty (in meters) was also recorded and included in the dataset.

Imaging

Image collection

Images were taken using a Canon EOS 5D Mark III camera and a Canon EF 100mm f/2.8 Macro USM lens (Figure 1, a).[2] Camera settings were manually optimized for macro imaging. An aperture of 2.8 was consistently used for all images to maximize depth of field, and ISO was constant at 200. Shutter speed ranged from 1/200 to 1/80, and was altered to increase for object-background contrast. The camera was remotely controlled by a laptop slave using the Canon EOS Utility 3 program (Figure 1, b).

The camera was mounted on a Cognisys Inc. StackShot Automated Focus Stacking Macro Rail, which in turn was mounted on a camera stand (Figure 1, c). The Stackshot Auto-Dist setting was used to standardize distance between image planes at 1 mm per step; the number of planes per imaged lot varied according to maximum sample height, and ranged from a minimum of 15 planes to a maximum of 64. Samples were illuminated using two Dolan-Jenner Fiber-Lite Model 181-Dual Gooseneck illuminators placed equidistant from the imaging stage (Figure 1, d). Vibration from these illuminators was minimal and did not affect image quality during the automated stepping process. However, use of the Fiber-Lites resulted in a color alteration of the specimens during preliminary imaging; to correct for this, the white balance 'tungsten' setting in EOS Utility 3 was used.[3]

High-throughput imaging techniques, modeled after Hull et al. methods (in prep) were utilized to maximize the efficiency of data collection. Imaging speed was increased by imaging lots as opposed to individual specimens, with a maximum of ∼150 individuals imaged per round.[4] Prior to imaging, pictures of a scale bar laid out in the x- and y-directions of the imaging plane were taken in order to calibrate the camera scale[5] for use during post-processing (Figure 1, e). This process was repeated at the beginning of every round of imaging (i.e. after the camera had been turned off or moved) to ensure that post-processing of images would result in accurate morphometric

---

[2]It should be noted that any camera capable of macro shooting can be used, as long as it produces "good enough" images. Desired image quality can be specified by the user.

[3]Color may not be constant throughout all images; as such, any analytical work requiring the use of color should be undertaken with caution.

[4]For organizational simplicity, the number of specimens per image was determined by the number of individuals in the lot being imaged.

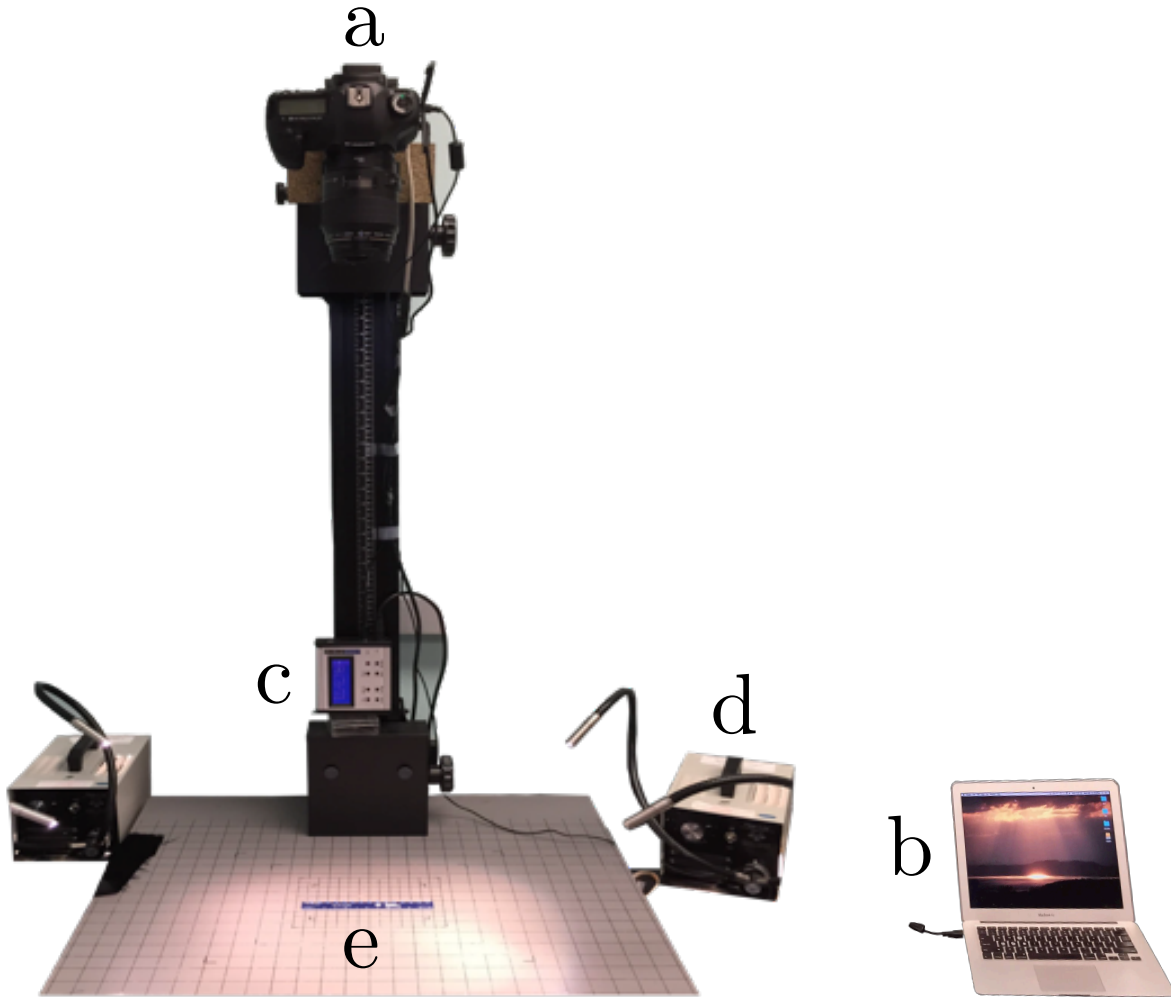[5]For the specimens used, this scale was in millimeters per pixel.

Figure 1: *The setup developed for high-throughput macroscopic imaging included: (a) a camera capable of macro shooting; (b) a laptop slave, which controlled the camera remotely; (c) an automatic stepper, which allowed for known distances between stacks, or planes, in the z-dimension, used to capture height; (d) appropriate lighting, and (e) a scale bar, used to retroactively calculate the scale (for this project, in millimeters per pixel for each image).*

extractions.[6] Specimens were laid out on a uniformly dark background—typically, a large black velvet cloth—in rows such that no individuals were touching. The StackShot automatic stepper produced a stack of z-slices that can be used to create an extended-depth-of-focus (EDF) image for each lot. The stacks can be used to extract images of each individual after the completion of imaging: namely, z-stacks can be utilized for creation of 3d height maps, and stacks can be

---

[6]It is important to note that this step is critical to any imaging process utilizing post-processing methods, as typical cameras are oftentimes not 'square'; that is, a given camera will likely not produce images with the same amount of pixels in both the x- and y-directions.

compiled into EDFs for 2d morphometric analysis. As such, each individual specimen is digitized, and provides a wealth of morphometric information in the process.

Image processing and analysis

Post-processing was completed using the Hull Lab Automorph software package (available online at people.earth.yale.edu/automorph/pincelli-hull or github.com/HullLab). The large number of individuals collected required that post-processing be done using a high-performance computing cluster, Grace (http://research.computing.yale.edu/grace), which allowed images to be batch-processed. The segmenting process (i.e. the extraction of individual objects from an image of a large grouping of specimens) utilized the `segment` software included in the Automorph Local package. `segment` was originally developed to identify objects from raw TIFF images, separate those objects into folders containing the full z-stack of object images, and label each object according to its museum catalog number and location as well as with basic imaging information (Hull et al, in prep). Labeling images using `segment` with catalog numbers, side IDs, and basic imaging information ensures that all images are permanently associated with the basic information need for re-analysis; as such, these images should allow for reproducibility as well as facilitate novel off-site research. The segmented z-stacks are later processed and combined into a single best 2d EDF image for each object using the `focus` software included in the Automorph Local package; these EDF images are labeled with the same information given in `segment`.

`segment` is a Python routine that identifies discrete white regions in a black-and-white image, chops these regions out of the raw z-stack slides, and saves the chopped stacks according to object number. In order to account for problems associated with using a camera rather than a microscope to take images, `segment` was modified into two versions: micro and macro-specific `segment`. Macro-specific `segment` includes a package, `prepare`, which ensures that any apparent zooming caused by camera motion through the z-dimension is eliminated. It works by resizing each image to the size of the bottom plane and ensuring that all images are aligned. `prepare` performs the following operations:

1. Rotates each plane to the orientation that the bottom plane by checking that the goodness of alignment is high (where $0 \leq$ alignment ≥ 1). If alignment is low, the current image is

rotated 180 degrees, and alignment is reassessed.

2. Scales the properly-oriented images to the size of the bottom plane. Again, goodness of alignment is checked to ensure that objects are aligned throughout the stack.

3. Places processed files in the parent directory. Original images are placed in a folder labeled 'unprocessed', and any intermediate files are deleted.

4. If directories have already been processed, `prepare` will abort.

5. Directories that have been previously processed can be reverted using a `--reset` flag.

Once images are appropriately rotated and scaled, thresholds, or grey-scale values used to delineate black and white in grey-scale images, are used to determine how successful segment is at finding all unique objects (Hull et al., in prep). Filters are used to set a range of acceptable object sizes, such that objects that are too small (e.g. dust, sand, etc.) or too large (e.g. accidental image borders) are excluded from `segment`'s analysis. `threshold` and `filter` are user-defined, and as such must be optimized by the user. `segment` operates as follows:

1. Users must specify whether `segment` should operate in `sample` or `final` mode. In `sample` mode, `segment` will box objects only on the bottom plane of the full-lot image, using a range of thresholds and filters input by the user. These images are labeled with their respective thresholds and filters, and are placed into a 'sample' folder. In `sample` mode, `segment` only follows steps 2-4.

2. Images are filtered using the user-specified threshold value and minimum/maximum size constraints.

3. Objects are identified using the difference in contrast between the desired object (typically, light-colored) and the background (typically dark).

4. Once identified, objects are boxed. Each box is labeled with a number, corresponding to the object number of each individual (Figure 3, page 19).

5. Boxes are cut out of the z-stack and placed into an object folder, such that each individual object folder will have the same number of stacks as the full-lot image.

6. Each plane in the stack is labeled with information pertaining to the object—i.e. its locality, age, and catalog numbers—as well as the version of the code with which it was processed. In addition, labels contain a scale bar, which is derived using the scaling constant (e.g. mm/pixel) for both the x- and y-directions. These scaling constants are user-defined.

Because the objects imaged—patellogastropods—approximate simple cones, a single `threshold` value of 0.16 was sufficient for the majority. In addition, the simplicity of the objects allowed `filter` to be constant for all images at `minimumSize = 3` pixels and `maximumSize = 2000` pixels. In addition, labels were user-defined, and reflected the age ("Recent"), locality (e.g. "Monterey, CA"), and catalog number of each lot (e.g. UCMP 130000), as well as where the images were processed (i.e. the Yale Peabody Museum), and by whom.

`focus` is a Python routine that batch processes each object's image stacks in Zerene Stacker. Zerene Stacker is additionally used to create new EDFs for objects; it generates a single-best EDF for each object within a slide, which can subsequently used for morphometric analysis (Hull et al., in prep). `focus` operates as follows:

1. Stacks are temporarily stripped of the labels provided by `segment`. Original stacks are saved in a folder called "z.stacks".

2. These unlabeled images are passed to Zerene Stacker, which runs in headless mode to batch focus each object's stacks into a single EDF (Figure 4, page 20).

3. Unlabeled EDFs are output to a folder called "focused_unlabeled".

4. EDFs are copied to a folder called "focused", and labels are re-added by object number.

5. A settings file and a log of Zerene Stacker's actions are output throughout the duration of `focus`, so that activity can be monitored.

Once all objects are focused (e.g. Figure 5, page 21), the Matlab routine `run2dmorph` is used to extract 2D shape parameters (e.g. major axis (length), minor axis (width), area, perimeter, rugosity, and height of specimens) and outline coordinates from black-and-white thresholded images (Hull et al., in prep). `run2dmorph` outputs a number of CSV files with morphometric data, and works as follows:

15

1. Users can specify a number of different parameters that pertain to image filtering and smoothing of the eventual outline extracted. Users can also choose to save intermediate (filtered) images to allow for diagnosis and correction of potential filtering problems.

2. Unlabeled EDFs are passed (in order) through a smoothing, RGB, greyscale, and black and white filter.

3. The final filtered image is used to determine the object's outline (Figure 6, page 22).

4. Each object's outline is placed on its respective EDF image to allow for a visual check of its fidelity. These images, along with all other outputs, are saved to a folder labeled "morph2d", which is nested inside of the "focused_unlabeled" folder. EDFs with outlines are labeled by lot and object number and end in "final.tif" (e.g. "UCMP_130000_obj00001_final.tif").

5. The coordinates of the outline are plotted and saved in an image (which is labeled by lot and object number and ends in "aspectratio.tif"), which also depicts aspect ratio.

6. Morphometric data is saved to four CSV files, all of which are prefixed with the ID number of the lot (e.g. "UCMP_130000"), and which end in "morph2dproperties.csv", "aspectratio.csv", "coordinates_original.csv", and "coordinates_smoothed.csv". These contain, respectively, morphometric measurements (e.g. axis length, area, rugosity, etc.), aspect ratio information, original coordinate positions, and coordinate positions after a smoothing factor (which is user-defined) is applied.

In addition to 2d morphometric analysis, 3d volumetric analysis is possible using the `run3Dmorph` function. Results were calibrated using both imaged (`run2dmorph`-processed) and manual measurements taken from a select number of lots. The formula

$$V = \frac{\pi}{3} \cdot a \cdot b \cdot h, \tag{1}$$

where a represents semimajor axis[7], b represents semiminor axis, and h represents height, was used to calculate volume for each of the test specimens. Using current imaging techniques, it was

---

[7]The semimajor axis is half the distance across an ellipse along its major ferret diameter, i.e. its long principal axes, while the semiminor axis is half of the distance across an ellipse along its minor ferret diameter, i.e. along its short principal axes

found that `run3dmorph` was only accurate at calculating volume for objects larger than 5 mm in height. Given this accuracy, `run3dmorph` was used to calculate volume for some but not all imaged specimens at the time of writing, and as such these were excluded from analyses.

Environmental covariates were incorporated into the dataset using an R protocol developed to extract temperature and cholorphyll a data hierarchical data format (HDF) files (Saulsbury 2016 pers. com.). HDFs containing MODIS Aqua oceanographic data for two months out of each year available were downloaded from the NASA Giovanni portal (http://giovanni.gsfc.nasa.gov/giovanni/). July was selected as it had lowest between-year standard deviation for chlorophyll and temperature data, and January was its counterpart. HDFs were then converted into TIFFs to allow for data extraction, and temperature and cholorphyll a data from 2002–2015 were extracted for each locality. These yearly values were then used to create January and July averages for the 13-year interval.

Figure 2: *A typical imaged lot where individuals are ordered in rows such that they are not touching other individuals. This placement is utilized to maximize the number of objects per unit area and minimize recognition error when using the Automorph package. This lot, UCMP 53343, locality 2770, is comprised of* Lottia pelta *from San Juan Island, WA.*
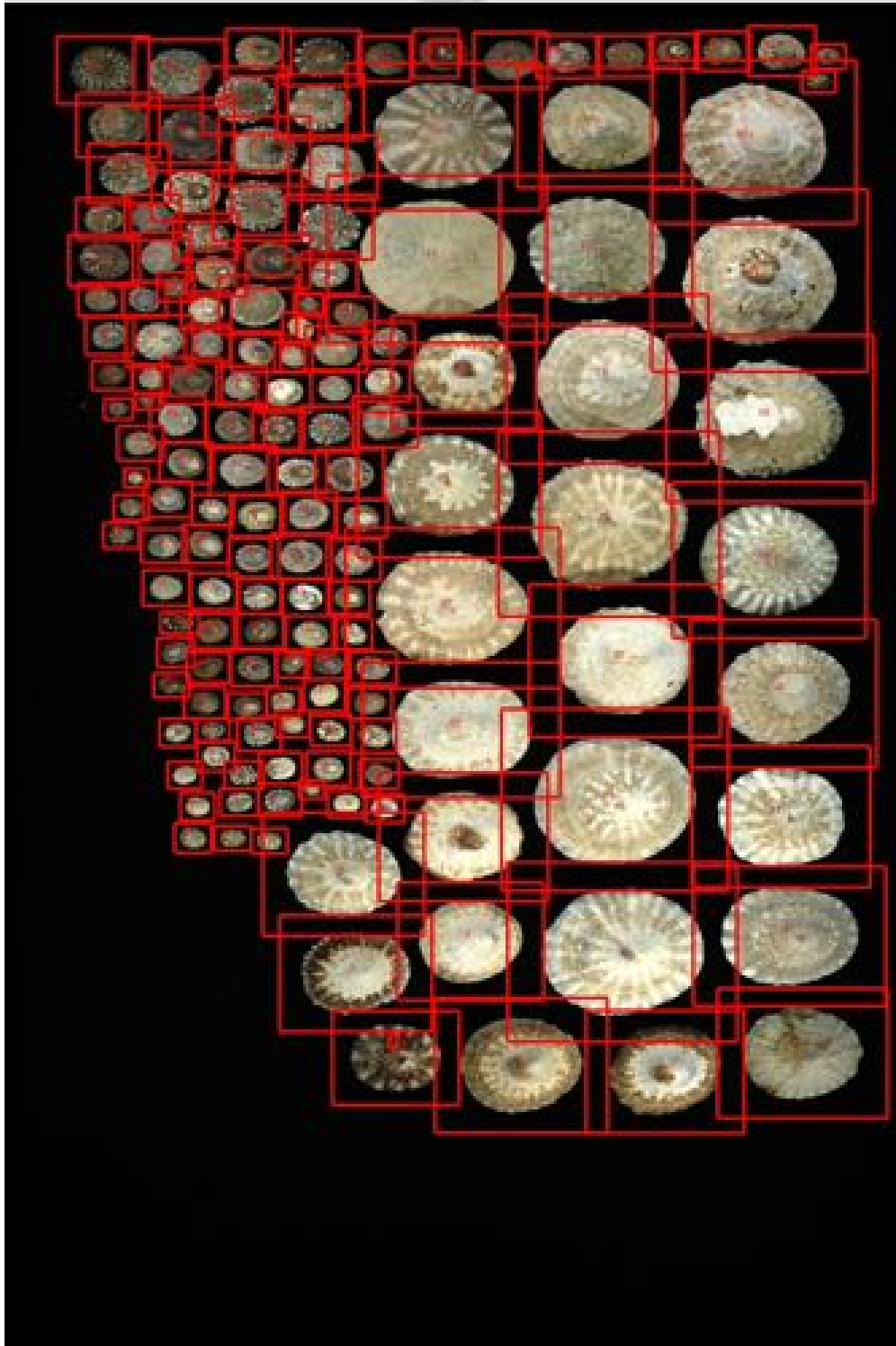
Figure 3: The same imaged lot as in Figure 2 (UCMP 53343, locality 2770) after processing with segment. Individuals are boxed in the full lot image, and labeled with their object numbers (typically, in the center of their respective box).
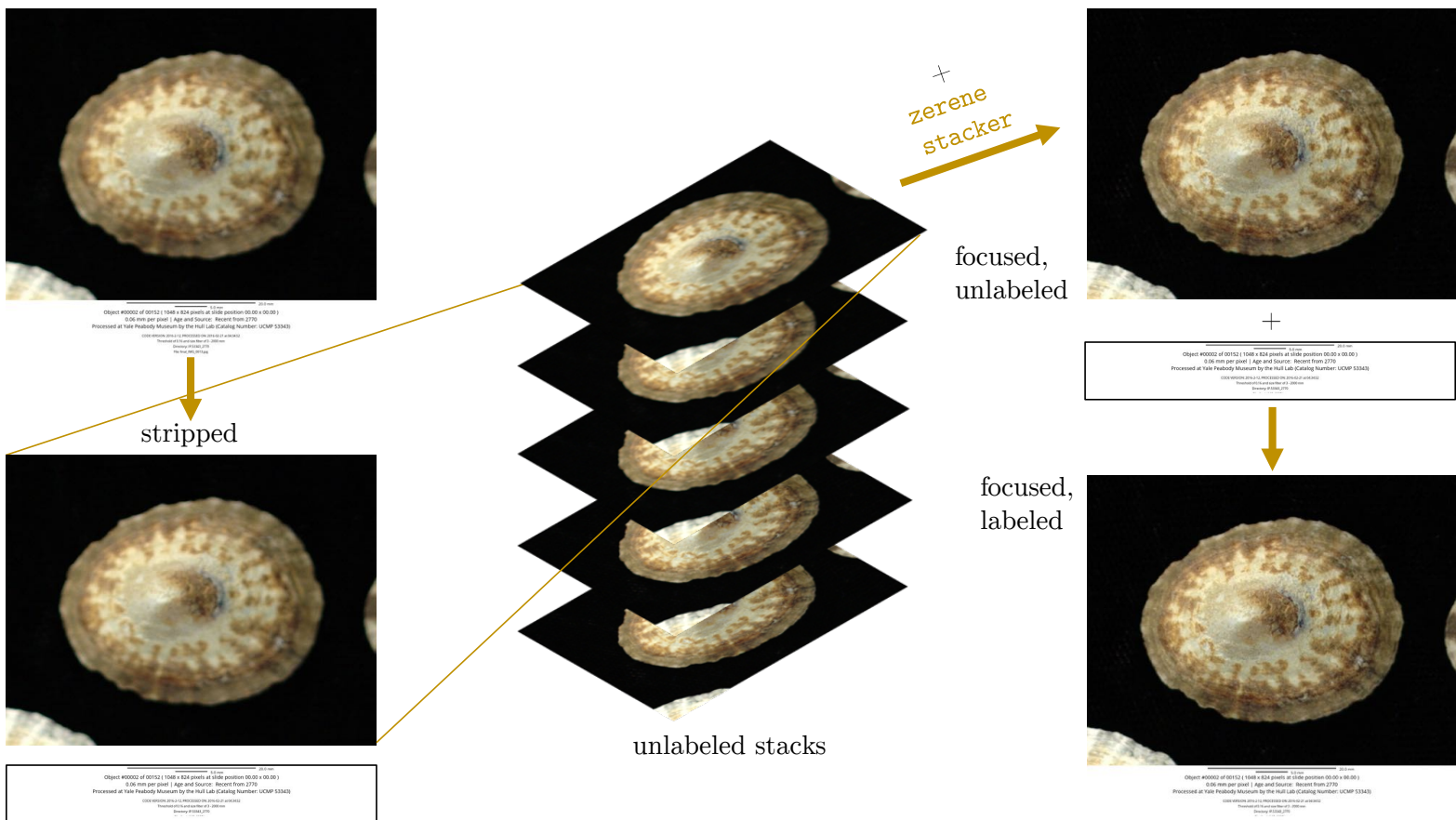
Figure 4: `focus` workflow: Each object's image stacks are stripped of their labels, and these labels are saved. Unlabeled stacks are then passed through Zerene Stacker, which creates an extended-depth-of-focus (EDF) image for the object stack. Labels are then re-added, resulting in a labeled EDF for each object.

Figure 5: A typical extended-depth-of-focus (EDF) image output by `focus`*, labeled with object, locality, and catalog information, as well as with a measurement of size (in mm/pixel), a scale bar, the version of code with which it was processed, and the threshold and filter defined by the user.*
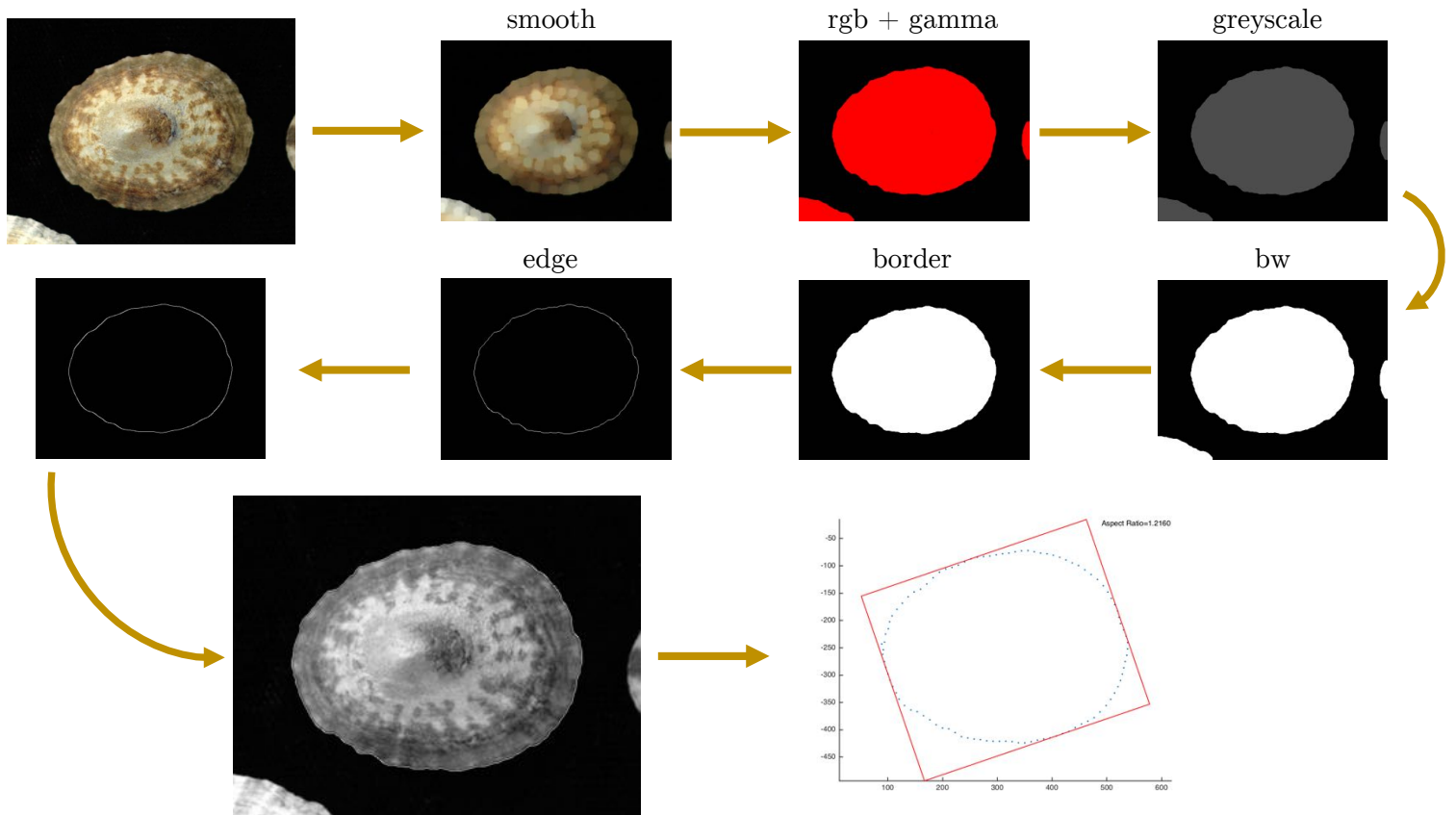
Figure 6: `run2dmorph` *workflow: each object's unlabeled image is passed through a series of filters, which work to extract the object's outline. Once the final outline is procured (shown on the far left of the middle row), it is placed on a lower-resolution image of the object (to aid visual checks), the outline's coordinates are plotted, and the aspect ratio is shown.*

Results

12,655 individuals, representing 29 species, were imaged over the course of 2 months. For each, 38 variables describing measurements of size, environmental covariates, locality, and catalog information were collected. Of these, 11,512 individuals had accurate locality information and extractable outlines. These individuals come from 296 unique sites, with a northernmost range limit at Cape Yakataga (60.06°N) and a southernmost range limit at Cabo San Lucas, Baja (22.90°N). Individuals were collected throughout the 20$^{\text{th}}$ century, and as such are of Recent age. Measured variables were major axis length (i.e. shell length), minor axis length (i.e. shell width), eccentricity, rugosity, shell area, perimeter, and aspect ratio (as well as the height and width of the enclosing rectangle). Environmental variables included January and July sea surface temperature and Chlorophyll a averages, as well as monthly averages, for all possible latitudes during the years 2002–2015.

Patterns in body size variation in communities and species

Body size tends to increase northward, but is poorly described by latitude. Shell area was considered to be the most representative measure of body size, especially given that length and width were found to scale linearly with area. Shell area ranged from 35.9 to 51764.6 mm^2 for all individuals, with a median at 1645 mm^2 and a mean of 2677 mm^2. Similarly, shell length ranged from 2.25 to 89.24 mm^2, and had a median of 16.32 and mean of 18.18 mm^2. Area was log transformed to account for heteroscedasticity in the raw data. When log(Area) was plotted across latitude, it was obvious that variation in size at each site is high (Figure 7, page 24). A linear regression for all individuals, using the formula log(Area) $\sim$ latitude, returned a weak tendency for body size to increase with latitude ($R^2 = 0.03$, $p < 2 \times 10^{-16}$)[8]. From this, it is evident that latitude alone does

---

[8]For all analyses, $\alpha = 0.01$.
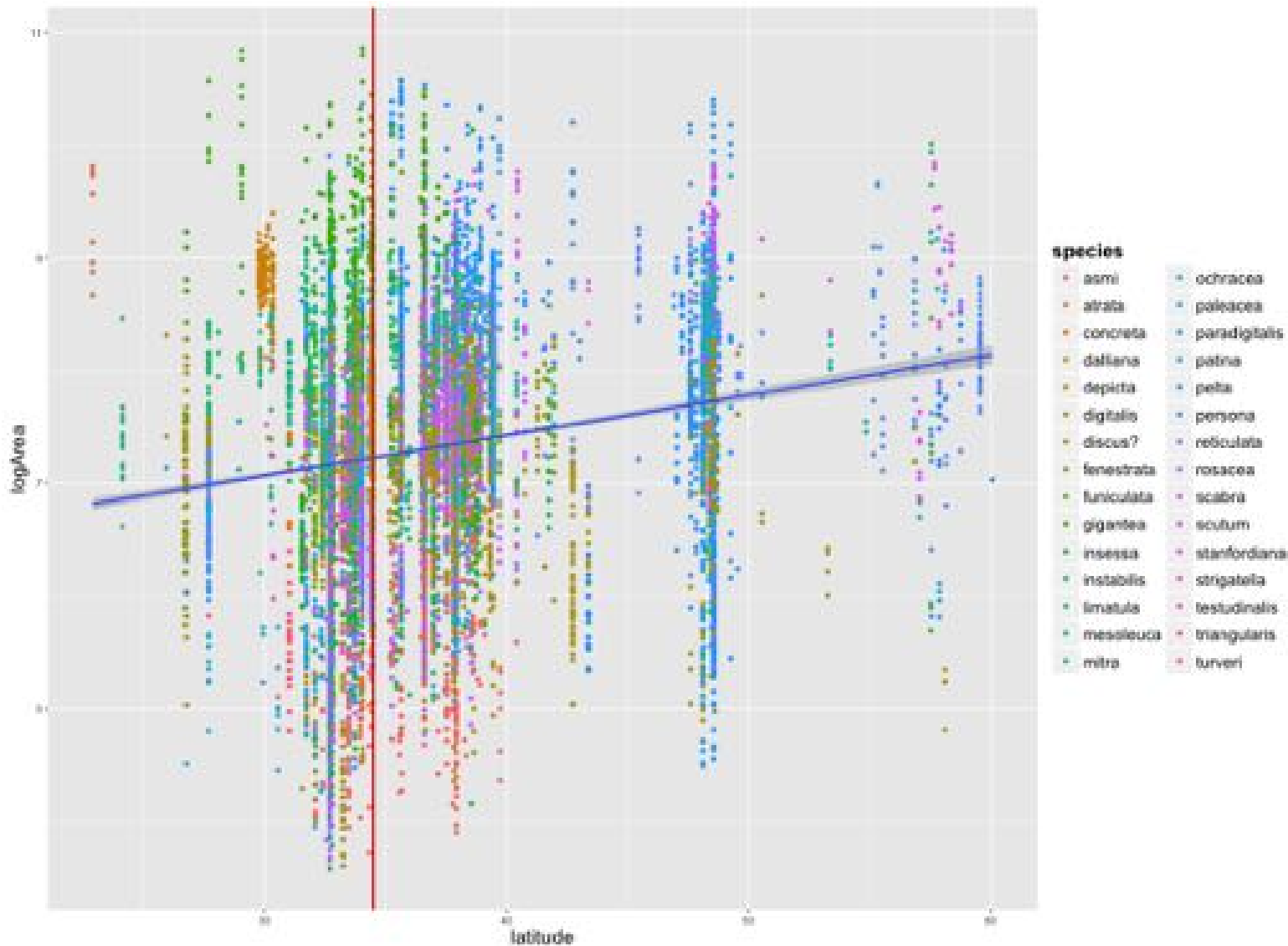
Figure 7: Body size (represented by shell area, and scaled logarithmically) across latitude. Points are colored by species, and a linear regression (using the formula logArea ∼ latitude) is shown in blue, with a 95% confidence bound in grey. The red line at 34.5° represents the provincial boundary at Point Conception, CA.

not explain the high variation in size present both within communities as well as across latitude. It is, however, apparent that there is a slight trend in assemblage size, with larger shell areas found more frequently towards the northern end of the distribution.

Community structure in the dataset roughly reflects that of natural communities. To determine whether dataset community structure reflects that of natural communities, community structure throughout the transect was assessed with cluster analyses. Data was placed into 1-degree latitu-

dinal bins, and two distinct analyses were performed: one using species' presence-absence data and the other using relative abundance of each species. Jaccard similarity coefficients were calculated for each group, and both groups were found to have 5 k-means clusters (Figure 8, page 33). There were 4 well-supported clusters, which roughly agreed with known provincial boundaries. In particular, the provincial boundary at Point Conception was highly supported. Given this, it appears that community structure is shown to vary in the sample approximately as it does in observed, naturally-occurring communities, and any community-level analyses should be fairly representative of natural trends.

Communities are appropriately sampled. While community clusters are representative of natural provincial boundaries, perhaps the data is under-sampled. To account for potential under-sampling, the data was subset to include only those latitudes (i.e. communities) that contained 10 or more individuals. This subsampled data resulted in a similar trend as the gross data: it demonstrated a weak increasing trend in body size across latitude, with a basic linear regression (log(Area) $\sim$ latitude) returning an R^2 of 0.03 ($p < 2 \times 10^{-16}$). These results held even when data was subsampled to include no less than 50 individuals per site. In addition, the minimum, maximum, median, and mean shell area of this subsampled data were nearly equivalent to those of the raw dataset. Minimum and maximum area were exactly equivalent, whereas the median and mean were only slightly lower at 1635 and 2649 mm^2, respectively. As such, it does not appear that under-sampling is a problem in this dataset.

Size trends within species are variable, but generally increase northward, and poorly track latitude. Intraspecific linear regressions, using the formula log(Area) $\sim$ latitude for species-specific subsets of the data, returned significant trends for the interaction of log(Area) and latitude for 16 species (Figure 9, page 34). Of these, 13 had weakly increasing trends in body size with latitude, and 3 had decreasing trends (Table 1). Species with increasing trends are widely varied in their ranges.[9] All but three cross the Point Conception provincial boundary, whereas two (*L. instabilis, L. scutum*) are exclusively found to the northern end of Point Conception, and one (*L. mesoleuca*) is found to the south of the provincial boundary. Of the three species that have decreasing trends in body size with latitude, two (*L. digitalis, L. pelta*) are found along the entire transect, with ranges from Alaska to Baja, California, Mexico. The third species (*L. dalliana*) is found exclusively to the

---

[9]Species ranges and descriptions can be found in the Appendix, page 54.

Table 1: *Intraspecific trends in body size, where trends are denoted as increasing in size with latitude (i.e. linear regressions with a positive slope) or decreasing in size with latitude (i.e. those with a negative slope). Linear regression output for each species with latitude as a significant predictor, using the formula log(Area) ∼ latitude. Asterisks denote species that are present at less than ten sites.*

Species	Size increase	Size decrease	R^2
Acmaea mitra	X		0.07
Lottia asmi	X		0.06
L. dalliana		X	0.22
L. digitalis		X	0.01
L. fenestrata	X		0.21
*L. funiculata**	X		0.11
L. insessa	X		0.24
L. instabilis	X		0.13
L. mesoleuca	X		0.12
L. paradigitalis	X		0.07
L. patina	X		0.41
L. pelta		X	0.02
L. persona	X		0.29
L. rosacea	X		0.39
L. scabra	X		0.07
L. scutum	X		0.06

south of Point Conception. It is obvious from the low R^2 values that a single-variable linear model does not explain the variation in body size observed. All pairwise additions of Chlorophyll *a* concentration to each species' linear model only weakly increased their explanatory power, while pairwise additions of temperature decreased their explanatory power. As such, environmental variables did not increase the goodness of fit of intraspecific linear models beyond a single predictor.

Are size patterns scale dependent?

Subsampling by province and species demonstrates that size patterns are likely scale-dependent. When the data is analyzed using the gross dataset, overall trends show an increase in body size with latitude. However, as demonstrated, this correlation is weak. In order to determine whether this trend holds at a finer resolution—namely, at the scale of faunal provinces (e.g. Californian & Panamic, Oregonian, and Arctic), as well as at a species level—groups were subsampled and body size trends were examined. When the data was subset into a southern group (i.e. the Californian & Panamic province, which lies below the provincial boundary at Point Conception) body size

follows a negative trend with latitude (Figure 11, page 36). Size-frequency distributions similarly demonstrate that provincial-level subsampling returns size structures with different means for each province.

Body size trends in subgroups

While size trends among provinces reflect general trends, size trends within provinces do not. Linear regression of body size by latitude for the well-sampled Californian and Panamic Provinces[10] (latitude $< 34.5°$N) returns a weakly negative trend, contradicting the regression trend depicted for the global dataset ($R^2 = 0.004$, $p = 9.96 \times 10^{-6}$; Figure 11, page 36). When poorer-sampled regions (i.e. the Panamic province, between 22.8 and 27.8°N) are removed, this negative trend is still apparent. Linear regression for the larger Oregonian province (34.5°N to 55.5°N) returned a weak increase in body size with latitude ($R^2 = 0.01$, $p = 4.73 \times 10^{-15}$), while the a linear regression for the Arctic province (55.6° to 60.1°N) found latitude as a non-significant predictor of body size. Shell area within the Californian and Panamic Provinces had a median of 1333 mm^2, and a mean of 2283 mm^2. As such, Californian & Panamic size is slightly less than overall size (Figure 12). In addition,

Figure 12: Size distributions by province.

between-province mean size is different, with the highest mean area in the Arctic[11] (4200 mm^2), the lowest in the Californian & Panamic Province, and the Oregonian mean (2992 mm^2) falling in between. As such, while regressions are inconclusive for the Arctic province, and return differing trends for the Californian & Panamic and the Oregonian provinces, the mean size among the groups increases northward.

---

[10]The Californian Province and the Panamic Province are grouped in this study for simplicity and denoted in figures as 'california' or 'californian' and referred to jointly as 'Californian & Panamic'.

[11]It should be noted that the Arctic is also the least well-sampled region, with 148 individuals, whereas the Californian and Oregonian provinces had 5366 and 5999 individuals, respectively.

Size-frequency distributions

Size-frequency distributions reinforce that trends differ when examined at finer scales. Size-frequency distributions (SFDs) were generated for all species using data regardless of sampling province (i.e. global data), as well as for each province (Californian & Panamic, Oregonian, and Arctic). These SFDs were calculated using individual-level body size data (i.e. raw individual body size measurements; Figure 13, page 37). Because these SFDs use empirical data, they should approximate actual body size distributions in each of the provinces. Two-sample Kolmogorov-Smirnov (KS) tests were performed to determine whether the individual-level distributions generated differed significantly. Using a two-sided distribution as the alternative hypothesis, each province was found significantly differ from the others ($p < 2.2 \times 10^{-16}$). In turn, they reflected the trends observed in Figure 12, with the lowest mean found in the Californian & Panamic province, and the highest in the Arctic.

Species-specific trends weakly reflect overall trends, and group trends are influenced by their position in the transect. intraspecific size-frequency distributions (SFDs) differ in terms of sample size, but demonstrate at a glance that size distributions across the transect (i.e. for global data) vary widely by species (Figure 10, page 35). While this is intuitive, it helps to demonstrate that species specifics do affect body size distributions across latitude. It is evident that some species' distributions are left-skewed, such that larger individuals are more prevalent. In particular, those species that have left-skewed distributions (e.g. *L. digitalis, L. gigantea, L. insessa,* etc.) are those that cross the Point Conception boundary (Figure 9, page 34). Taking this into account, data was subset into exclusively southern groups and exclusively northern groups (i.e. those that do not cross the provincial boundary) as well as into a subset of specimens that exist across the Point Conception boundary. Body size for exclusively southern groups has a minimum of 121.5 mm^2, a maximum of 18190 mm^2, a median of 4188 mm^2, and a mean of 4577. A total of 8 species and 283 individuals are represented in this group. In addition, 3 species are exclusively northern; however, these species were represented by 8 individuals, and as such their sizes were likely not representative. Species that cross the Point Conception boundary, i.e. those that occur in both southern and northern ranges, had a minimum and maximum body size equivalent to that of the raw data, and a median and mean of 1610 and 2630 mm^2, respectively. This group is composed of 19 species and 11222 individuals. A two-sample t-test returns that the exclusively southern

species' body size distribution is significantly different (and tends to be larger) than that of the cosmopolitan group. This trend seems to confirm that the resolution at which data is collected and analyzed affects the apparent size trends found.

Patterns in the underlying environment

The Eastern Pacific experiences a strong environmental gradient. The latitudinal gradient along the Eastern Pacific is particularly strong for sea surface temperature (SST) and Chlorophyll *a* (CHL) concentration. SST is particularly variable along the California coast, as it makes a nonlinear jump at the Point Conception provincial boundary, from 18°C to approximately 12°C. This boundary, then, is not only biological, but serves doubly as an environmental break, as it delineates the warmer southern environments from the cooler northern ones. As such, species that cross this break are subject to rapid and dramatic temperature change. CHL concentrations are less dramatic, particularly along the coastline of North America. CHL is seasonally variable across the transect, with a more heterogenous mode occurring during the summer months, whereas homogenous modes peak during the months of May and November (Thomas 2012).

    Environmental variables strongly track latitude. January average SST is highly correlated with latitude ($R^2 = 0.96$, $p = 2.2 \times 10^{-16}$), reflecting the increase in heterogeneity expected during the winter months, when differences in available sunlight between the poles and the equator are greater. July temperature average is less correlated with latitude ($R^2 = 0.46$, $p = 2.2 \times 10^{-16}$), which is to be expected given summertime thermal homogenization. These data demonstrate that temperature linearly tracks latitude, especially during winter months when thermal gradients are more pronounced. CHL also tracks latitude, though less tightly. July CHL average (i.e. the month during which CHL heterogeneity should be strongest) is a significant predictor of latitude ($R^2 = 0.43$, $p = 2.2 \times 10^{-16}$). January CHL average is also a significant predictor, though weaker at explaining variation in latitude ($R^2 = 0.23$, $p = 2.2 \times 10^{-16}$), which is to be expected given the homogeneity typically seen during cooler months (Thomas 2012). As such, CHL is fairly well correlated with latitude, especially during summer months when light is less of a constraint. Given this data, it appears that environmental variables track latitude nearly linearly (or, in the case of

January SST, perfectly linearly).[12]

Drivers of local body size variation in limpets

Environmental variables do not explain body size variation; instead, species composition is the dominant factor in determining local size distributions. Given that body size is highly variable, models were fit to the data in an attempt to explain whether body size variation is driven by environment or community structure (e.g. species present, and where). Temperature is not a good predictor of body size, nor is CHL. This may be because, as discussed, environmental variables track latitude, and as such do not add sufficient information to the model. However, latitude very poorly explains body size variation; instead, the species present, as well as provincial faunal groups, add a large amount of explanatory power to models.

Modeling

Environmental variables do not increase the explanatory power of linear models. Data was analyzed using stepwise, additive fitting of general linear models (GLM) and general linear mixed effects models (GLMM). Basic linear regression for all individuals, irrespective of province, using the formula logArea $\sim$ latitude, returned a weakly positive trend ($R^2 = 0.03$, $p = 2.2 \times 10^{-16}$; Figure 7, page 24). When sea surface temperature (SST) is added in to the linear model (with the formula logArea $\sim$ latitude + January temperature average), temperature is insignificant, and the R^2 value remains at 0.03 ($p = 0.0075$ for latitude). When Chlorophyll a concentration is accounted for (using the formula logArea $\sim$ latitude + January chlorophyll average + July chlorophyll average) all predictors are significant, but the R^2 is again 0.03 ($p = 1.19 \times 10^{-13}$, 0.0011, and 0.00058, respectively). When latitude, temperature, and chlorophyll are combined into a single linear model in an attempt to explain variation in body size, all variables but temperature are significant predictors but the resulting R^2 value remains at 0.03.

Accounting for community structure hugely increases goodness of fit. ANOVA was then performed to asses whether community structure explained additional variation in body size across latitude for all data (Table 2). Species present and faunal provinces, as well as the interac-

---

[12]It should be noted that the dataset does not capture daily and seasonal variability particularly well, but it does provide a nice, long-term "snapshot" of the region's trends.

tion between the two, were found to significantly explain variation in body size, or shell area (p $< 2.2 \times 10^{-16}$). However, a large amount of variation was left unexplained by the model. In light of this, ANCOVA was performed to determine whether a single-variable linear model (log(Area) $\sim$ latitude) provided a similar fit to this more complex model (log(Area) $\sim$ latitude + species + province + species*province). ANCOVA returned a significant difference between the two models (p $< 2.2 \times 10^{-16}$), indicating that accounting for species and province differences, as well as the interaction between the two, does increase the ability of the model to describe variation in body size.

Table 2: ANOVA table for all data.

	DF	Sum Sq	Mean Sq	F value	Pr(>F)
latitude	1	450.8	450.79	664.202	$< 2.2 \times 10^{-16}$
species	29	5730.6	197.61	291.156	$< 2.2 \times 10^{-16}$
province	2	147.9	73.94	108.937	$< 2.2 \times 10^{-16}$
species:province	27	699.6	25.91	38.176	$< 2.2 \times 10^{-16}$
residuals	11453	7773.1	0.68		

Subsetting the data returns a similar trend—community structure largely determines body size. This process was then repeated for the well-sampled Californian Province. ANOVA returned that species and latitude were highly significant predictors of body size variation (Table 3). An AN-COVA comparing the basic model (with just latitude as a predictor of body size) with the model incorporating species as a predictor returned that the second model significantly reduced the residual sum of squares. However, as with the previous model, a large amount of variation was left unexplained.

Table 3: ANOVA table for the Californian Province.

	DF	Sum Sq	Mean Sq	F value	Pr(>F)
latitude	1	35.1	35.14	58.78	2.081×10^{-14}
species	26	4409.1	169.582	283.64	$< 2.2 \times 10^{-16}$
residuals	5338	3191.4	0.598		

Linear mixed effects models confirm that species and province are the best predictors of body size. While these more complicated linear models explained a larger amount of variation in body size than a basic linear model (for the more complex model, the R^2 value is 0.47), the data only approximates a normal distribution, and as such linear mixed models were deemed more appropriate. A simple

linear mixed model, with species as a random effect and latitude as the only fixed effect, was applied to the data using the formula

$$\log(\text{Area}) \sim \text{latitude} + (1|\text{species}). \tag{2}$$

A Jarret Byrnes test and a Xu test (Xu 2003) for the effect size of the model both returned an R^2 value of 0.43. When compared to a null model, which removed latitude as a fixed effect, it was found to have a significantly better fit. When province was added in as a random effect and the two models were compared using ANCOVA, the second model improved significantly. Species diversity, which was calculated using relative abundance at 1-degree latitudinal bins, was then added to the model. This new model, which used the formula

$$\log(\text{Area}) \sim \text{latitude} + (1|\text{species}) + (1|\text{province}) + (1|\text{diversity}), \tag{3}$$

was compared to the linear mixed model with province and species as random effects using ANCOVA and found to significantly reduce the residual sum of squares. However, this model returned only a marginally better R^2 value of 0.45.[13]

Adding in environmental data does not improve the model. When temperature was added in as a fixed effect (for sites for which there were temperature data), using the formula

$$\log(\text{Area}) \sim \text{latitude} + \text{January SST average} + \text{July SST average} + (1|\text{species}) + (1|\text{diversity}), \tag{4}$$

Jarret Byrnes and Xu tests returned R^2 values of 0.45. Similarly, when Chlorophyll *a* concentration was added in as a fixed effect (for sites for which data was available), using the formula

$$\log(\text{Area}) \sim \text{latitude} + \text{January chla average} + \text{July chla average} + (1|\text{species}) + (1|\text{diversity}), \tag{5}$$

Jarret Byrnes and Xu tests returned R^2 values of 0.43. When the two environmental variables were combined in a single model, the resulting R^2 value returned was equivalent to the single environmental variable models.

---

[13]It is debated whether R^2 values are appropriate in determining the goodness of fit of linear mixed models; see Nakagawa and Schielzeth 2013.
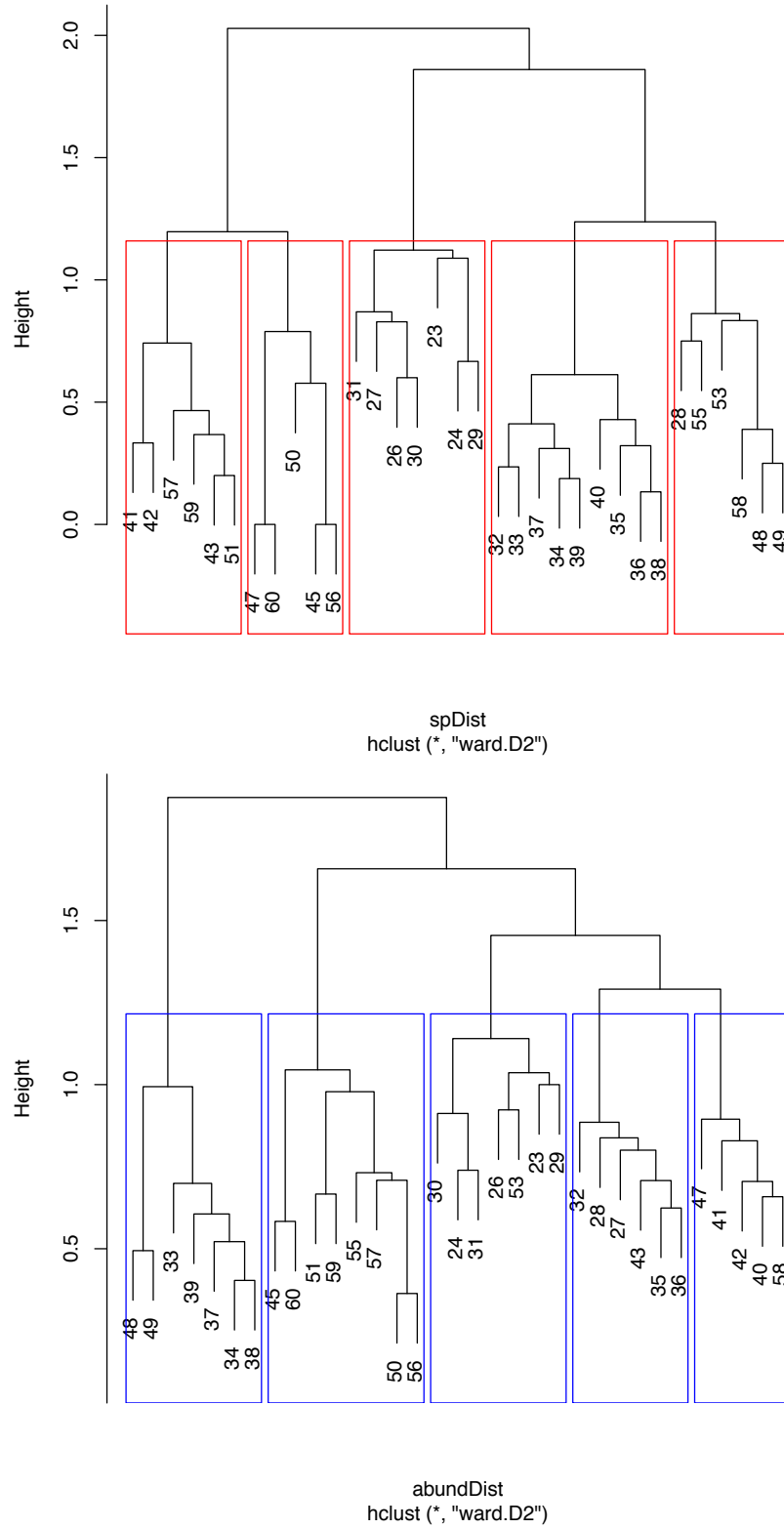
Figure 8: Cluster dendrograms for species community similarities across 1-degree latitudinal bins. The top dendrogram shows the similarities for communities constructed using presence and absence of species, whereas the bottom dendrogram shows similarities for communities constructed using relative abundance of species.
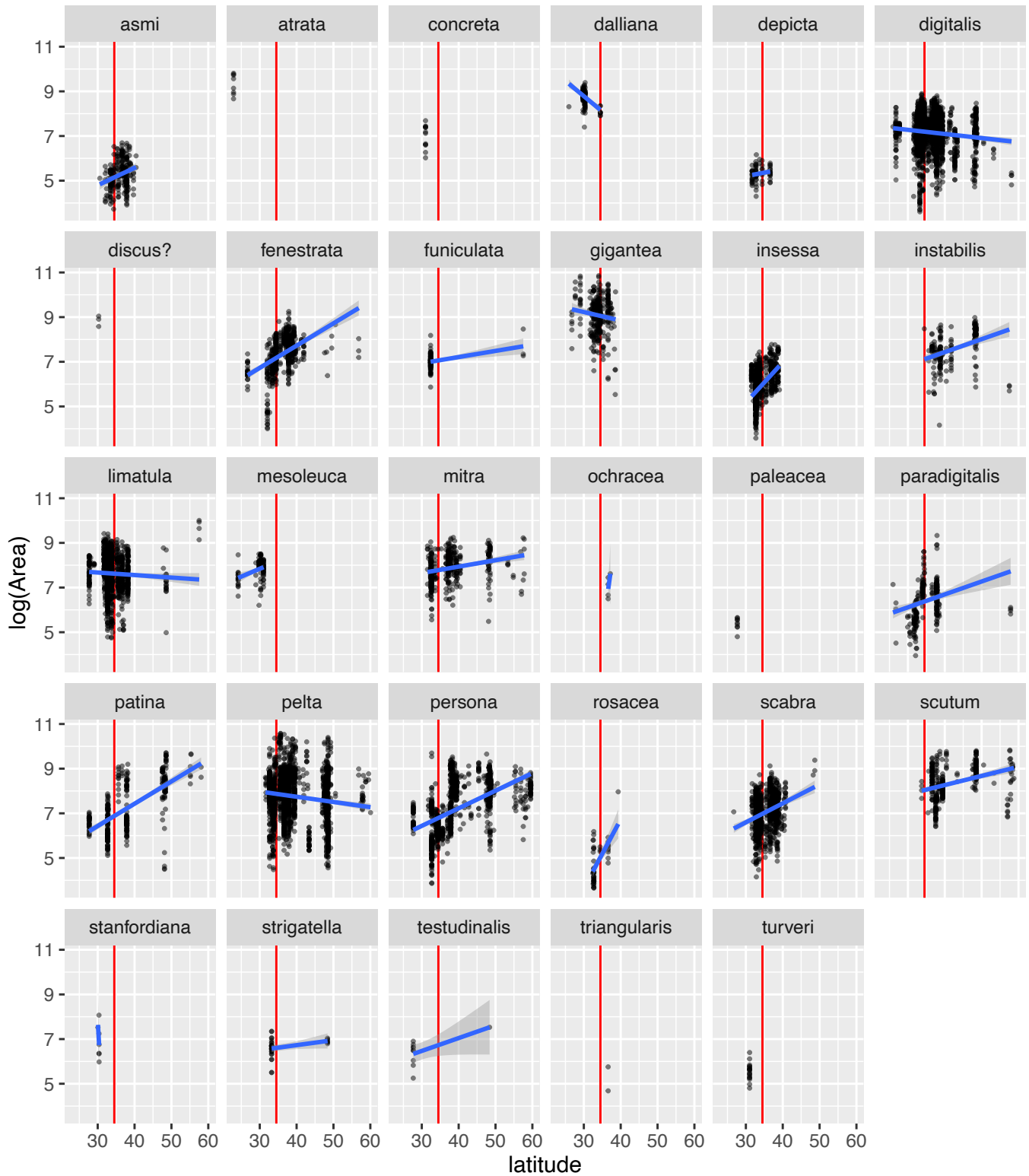
Figure 9: intraspecific trends in size across latitude. Each quadrant represents species-specific size-latitude trends, with red lines signifying the Point Conception provincial boundary at 34.5°N. Some species are poorly sampled, and are only represented at a few sites.
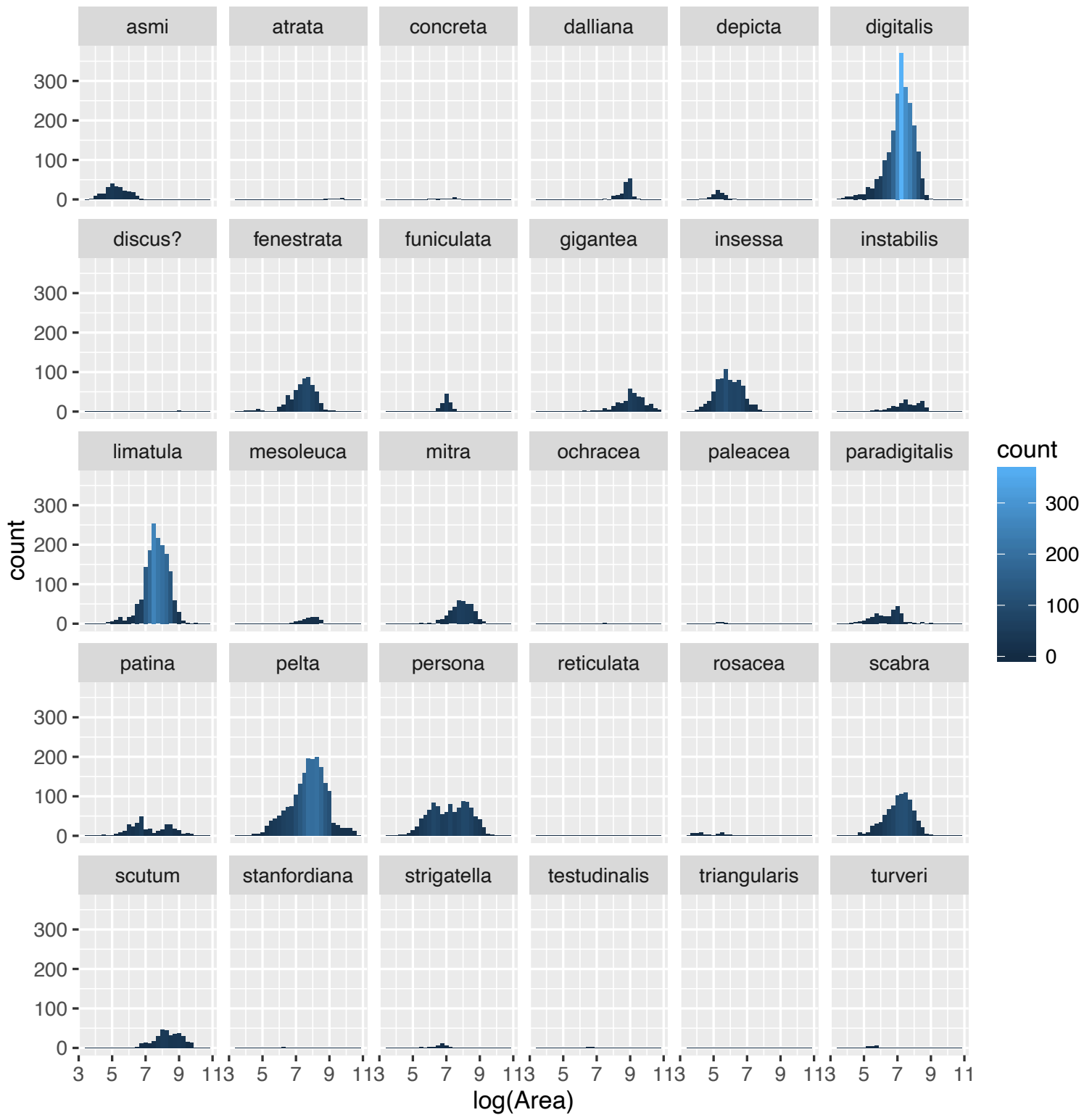
Figure 10: Species-specific size-frequency distributions for all data, i.e. not taking provinces into account.
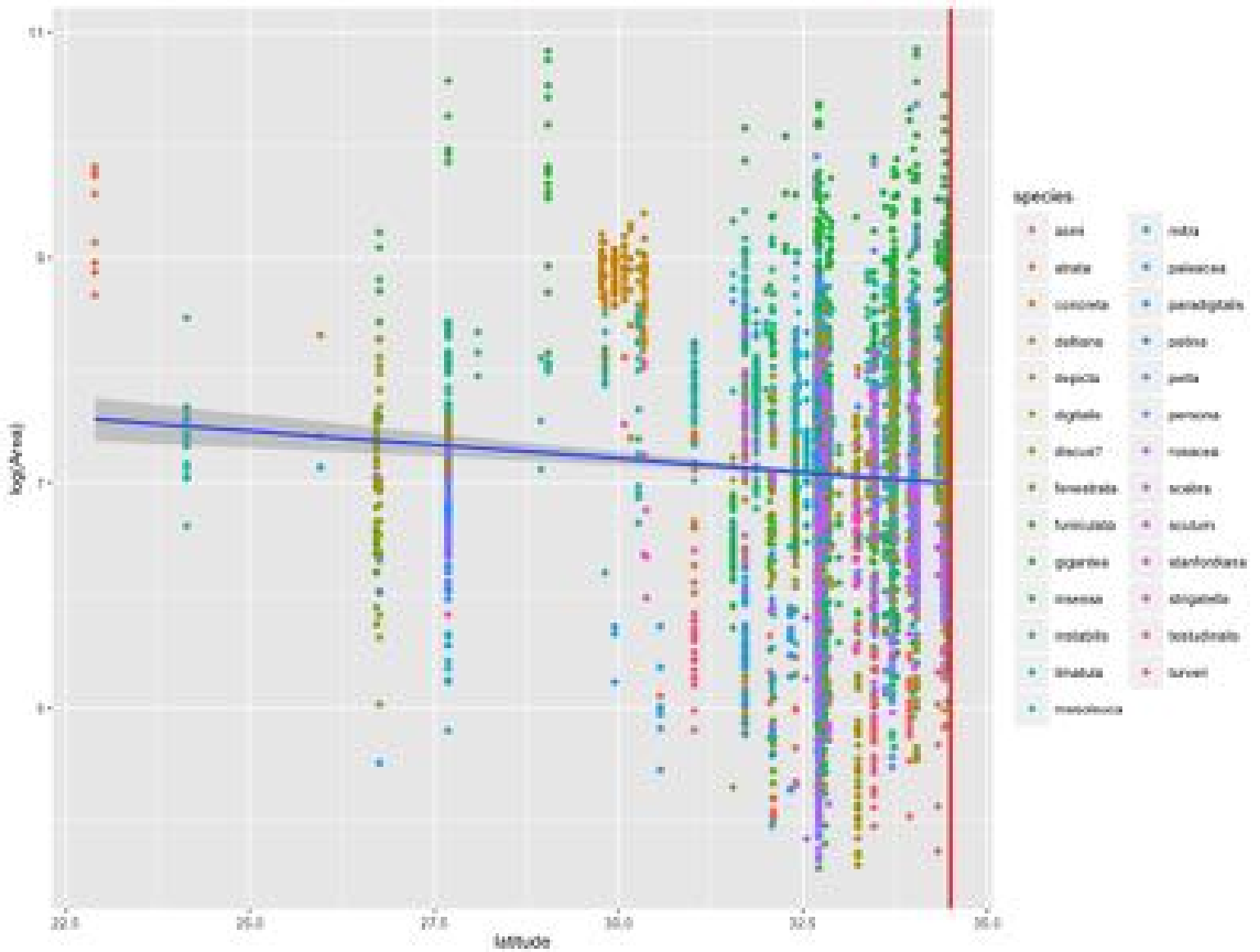
Figure 11: Body size across latitude for the Californian and Panamic Provinces (defined for this study as 22.8°N to 34.4°N). Points are colored by species, and a linear regression (using the formula logArea ~ latitude) is shown in blue, with a 95% confidence bound in grey. The red line at 34.5°N represents the provincial boundary present at Point Conception, CA.
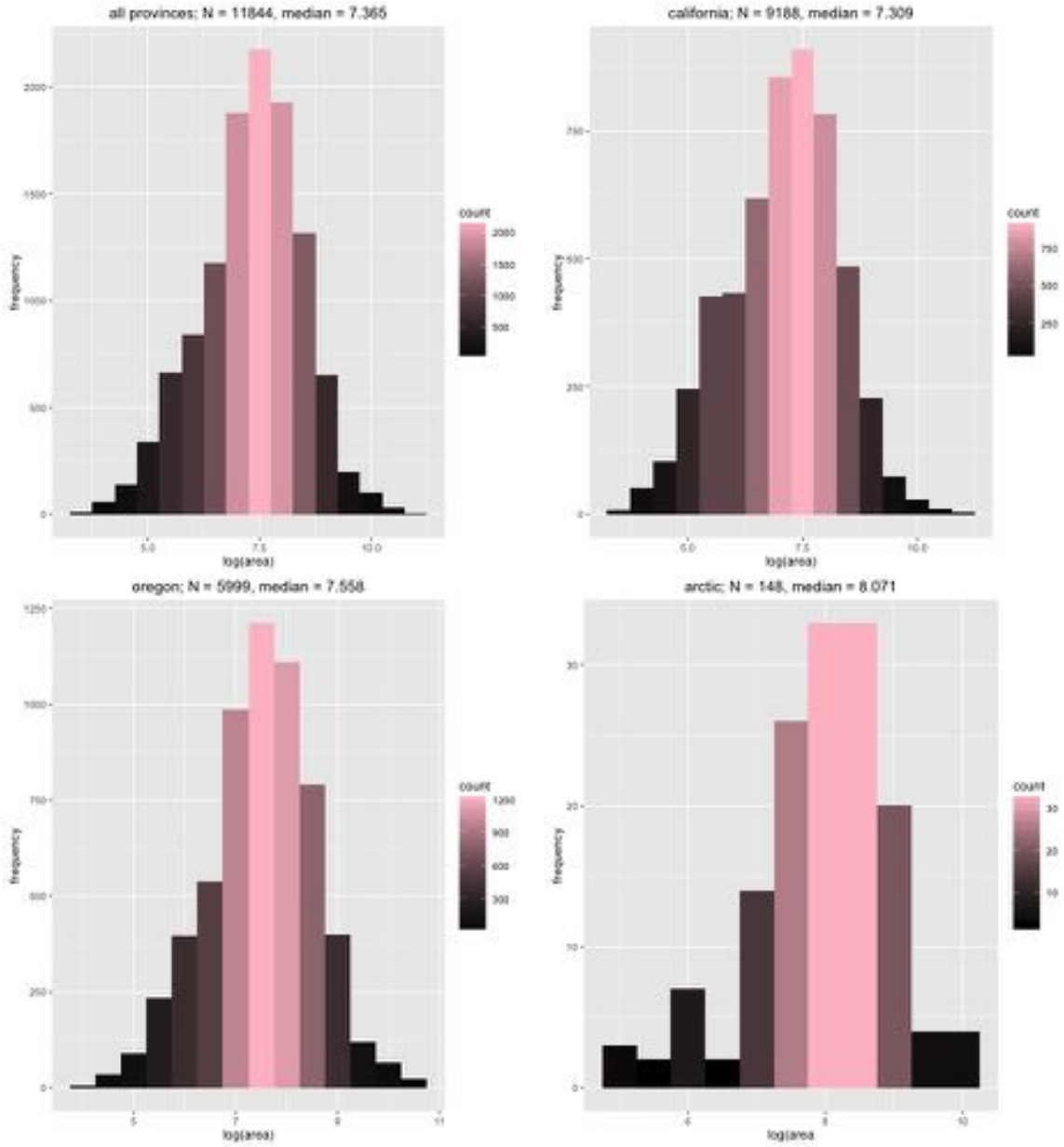
Figure 13: Size-frequency distributions generated using individual-level body size data, subset by province. N = the number of individuals in each province, where log(Area) is empirically observed.

Discussion

This dataset is the largest collected at an individual level for Patellogastropoda, and may also be the largest individual-level dataset for Mollusca. Given its size, as well as the depth of information it contains, it can help to answer a large number of questions. Only a subset of questions are tackled in this study, but they aim to provide a basic understanding of body size across space, for both inter- and intraspecific distributions. Here we examine whether individual-level data sheds new light on old biological problems; in particular, we attempt to deconstruct the trends in body size across communities, as well as the drivers of these trends.

Community and intraspecific patterns in limpet body size

Northeastern Pacific Patellogastropoda show a tendency to increase in body size with latitude. This broad assemblage trend takes individual variation into account, and demonstrates that, at a general level, Bergmann's rule holds for the patellogastropod group. However, it is apparent that while there is a general tendency for body size to increase poleward, latitude is a very poor descriptor of this trend, as it explains around 3% of the total variation in body size. Thus, while this group can be said to have a Bergmanian distribution, as it does get larger towards the poles, this size change is not *driven* by latitude, as Bergmann's rule seems to imply. As such, it appears that Patellogastropoda is a group that follows Bergmann's rule, but for very un-Bergmann reasons.

Of course, this finding—that latitude is an incredibly poor predictor of body size—requires examination of potential sampling biases in the data. Perhaps certain latitudes are more highly represented than others, and thus skew variability in such a way as to decrease the explanatory power of latitude. However, when the data is subset both by sampling province (e.g. 'California') as well as by a threshold cutoff of the number of individuals represented at each latitude, the finding

that environment is a poor predictor of body size holds. Community structure, in addition, clearly reflects that of natural communities, particularly as the provinces found in the dataset roughly match provincial boundaries observed in natural communities. The data, then, are representative. As such, it holds that body size increases for the group as a whole, but an individual's position in a latitudinal transect does not explain this trend. In fact, the amount of variability contained within a single latitudinal degree is greater than the variability in mean across latitudes. This means that even within relatively homogenous environments, patellogastropod body size is highly variable. The scatter in the data itself points to non-abiotic drivers of body size variation.

Intraspecific trends are much more variable than overall assemblage trends. Only half of all species have significant trends in size with latitude, but the majority of these increase in size towards the poles, mirroring assemblage size. Latitude proves a better predictor of body size for individual species, but still does a poor job at explaining overall variation. It does not appear that these trends are correlated with faunal provinces, nor with whether species ranges cross the Point Conception faunal (and environmental) break. Species-specific size-frequency distributions are similarly uncorrelated with provincial patterns. However, splitting species into exclusively northern-dwellers (i.e. those that have ranges with southern maxima above Point Conception) and southern-dwellers, as well as into those that span the Point Conception boundary, shows that southern-dwellers are significantly larger than the cosmopolitan group. (Northern-dwellers were too poorly sampled to be considered.) What this means is that species that exist exclusively below the Point Conception boundary are much larger than would be expected given the general Bergmanian trend observed for the overall group. This seems to contradict the finding that size increases with latitude, and hints at species-specific trends that differ from, and may underly, this general trend.

What both the assemblage and intraspecific trends demonstrate is that body size does generally increase northward, but it is unclear how species-specific trends compound to create this overall increase. It does not appear that all species' trends agree with this broader tendency to be larger at high latitudes. Only half of them have trends at all, and of these, the strength of their tendency to increase size with latitude varies widely. In addition, it is difficult to determine what those species that agree with the positive trend have in common, as well as what those that go against it share. A majority of species that have significant trends cross the Point Conception faunal and environmental break, but given that the majority of *all* species cross this break, this correlation

likely does not explain the variation in the data. As of now, what can be conclusively drawn from this data is that there *is* a size trend that corresponds to latitude, but that it is weak and exists only at a broad, general level.

Body size trends: a matter of scale

This conclusion necessarily requires analysis of whether the resolution (or scale) of the data affects the quality and level of information gleaned from it. Subsetting the data demonstrates that scale makes a large difference in the outcomes of body size analyses. It is particularly obvious that the applicability of Bergmann's rule depends highly on the resolution with which it is investigated. When looked at generally, without taking species differences or provincial boundaries into account, Bergmann's rule applies for the Patellogastropoda. However, the general trend changes when observed for a subset of the data, e.g. for the Californian & Panamic province, which shows a decreasing trend in body size with increasing latitude. Of course, this change in trend from global to provincial may result from either sampling or scale biases. That is, the California[14] province displays an opposite Bergmann trend when examined alone, while the dataset as a whole follows a traditional Bergmanian distribution, and this may not be representative. Perhaps the California province is well-sampled, and it is depicting a trend that may be obscured by poorer sampling for the global distribution. This is unlikely, however, as subsetting the data to include only those localities with large numbers of individuals (i.e. > 50 per site, irrespective of province) returns the same, opposite-of-general trend. In addition, if sampling bias is inherent in the collection, it is more likely to cause all distributions to homogeneously shift in comparison with natural populations. This is due to the elimination of smaller specimens, which is unlikely to disporportionately affect provincial size distributions. Thus, while sampling bias is always a problem when using museum collections, this observed opposite-Bergmann trend may reflect the actual structure of California communities. That is, while global trends reflect a Bergmanian distribution, the California trend is opposite, and these findings both appear robust to sampling bias.

In order to further deconstruct the effects of scale on perceived trends, we performed additional tests that began with coarse-resolution data using species exemplars, and were subsequently applied

---

[14]From here, 'California' refers to both the Californian province (27.8 to 34.5°N) and the part of the Panamic province included in this study (22.8 to 27.8°N), or both Southern and Baja California.

for data of successively finer resolution. Most studies that have investigated trends in body size in communities to-date have used a single exemplar measurement of a species typical (or maximum) body size. With individual-level measurements in patellogastropods, we can test the influence of this approach on the inferred patterns and determinants of community body size by generating distributions using increasingly better measurements. At the coarsest scale, distributions were generated across the transect using global exemplar measurements (Figure 14, page 42), which took the overall maximum size of each species and applied that size across the species' range (i.e. the number of observations equals the number of species in each province, per Roy et al. 2000). Following this, distributions were generated using provincial exemplar measurements (i.e. the provincial maximum size of each individual, where n = the number of species in each province; Figure 15, page 43) as well as using provincial exemplars weighted by the number of individuals in the raw dataset (i.e. relative abundance; Figure 16, page 44). Two-sample Kolmogorov-Smirnov (KS) tests were then performed to determine whether provincial datasets generated at each resolution (with a global mean, provincial mean, weighted provincial mean, or individual body size measurements) differed significantly. Using a two-sided distribution as the alternative hypothesis, distributions were not significantly different at the global and provincial level. However, two distributions were significantly different when using provincial, weighted data (California and Oregonian, as well as California and Arctic), whereas all distributions significantly differed when using individual-level data (Table 4).

What these analyses demonstrate is that resolution—i.e. whether individual measurements or

Table 4: Kolmogorov-Smirnov tests for each province. The resolution of body size measurements increases down the first column, from coarse (global exemplar measurements) to fine (individual measurements).

	California-Oregonian	Oregonian-Arctic	California-Arctic
global	D = 0.055, p = 1	D = 0.43, p = 0.14	D = 0.39, p = 2.20
provincial	D = 0.28, p = 0.24	D = 0.25, p = 0.68	D = 0.28, p = 0.50
provincial, weighted	*D = 0.14, p = 0.001*	D = 0.20, p = 0.20	*D = 0.27, p = 0.03*
individual	*D = 0.15,* $p < 2.2 \times 10^{-16}$	*D = 0.24,* $p = 1.3 \times 10^{-7}$	*D = 0.37,* $p < 2.2 \times 10^{-16}$
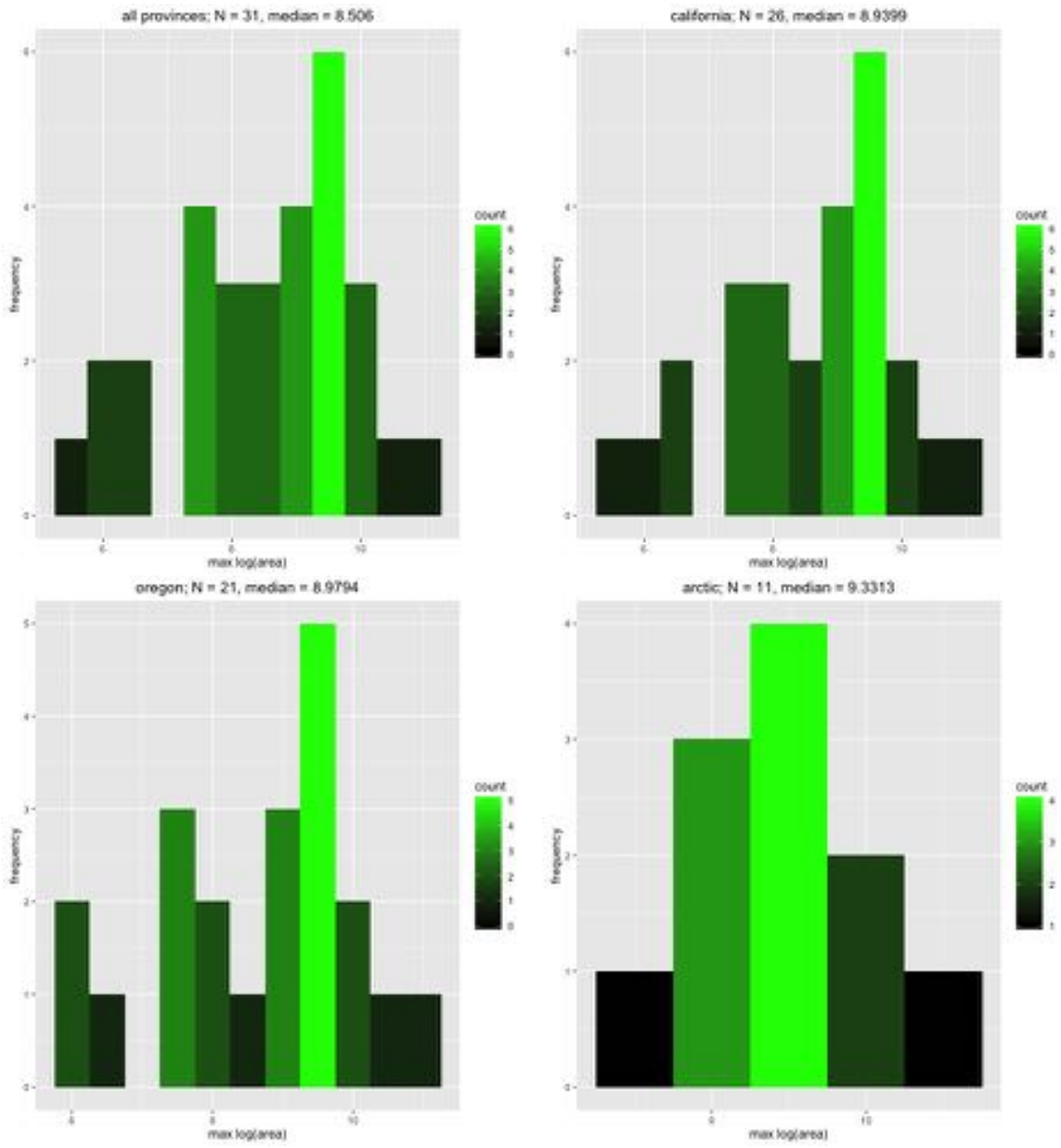
Figure 14: Size-frequency distributions generated using a global maximum for each species applied across their respective ranges. N = the number of species in each province, where max(logArea) is taken from the global distribution but applied only for species present in each province.

Figure 15: Size-frequency distributions generated using a provincial maximum for each species, applied n times, where n is the number of individuals present for each species. N = the number of individuals in each province, where max(logArea) is taken from provincial distributions.
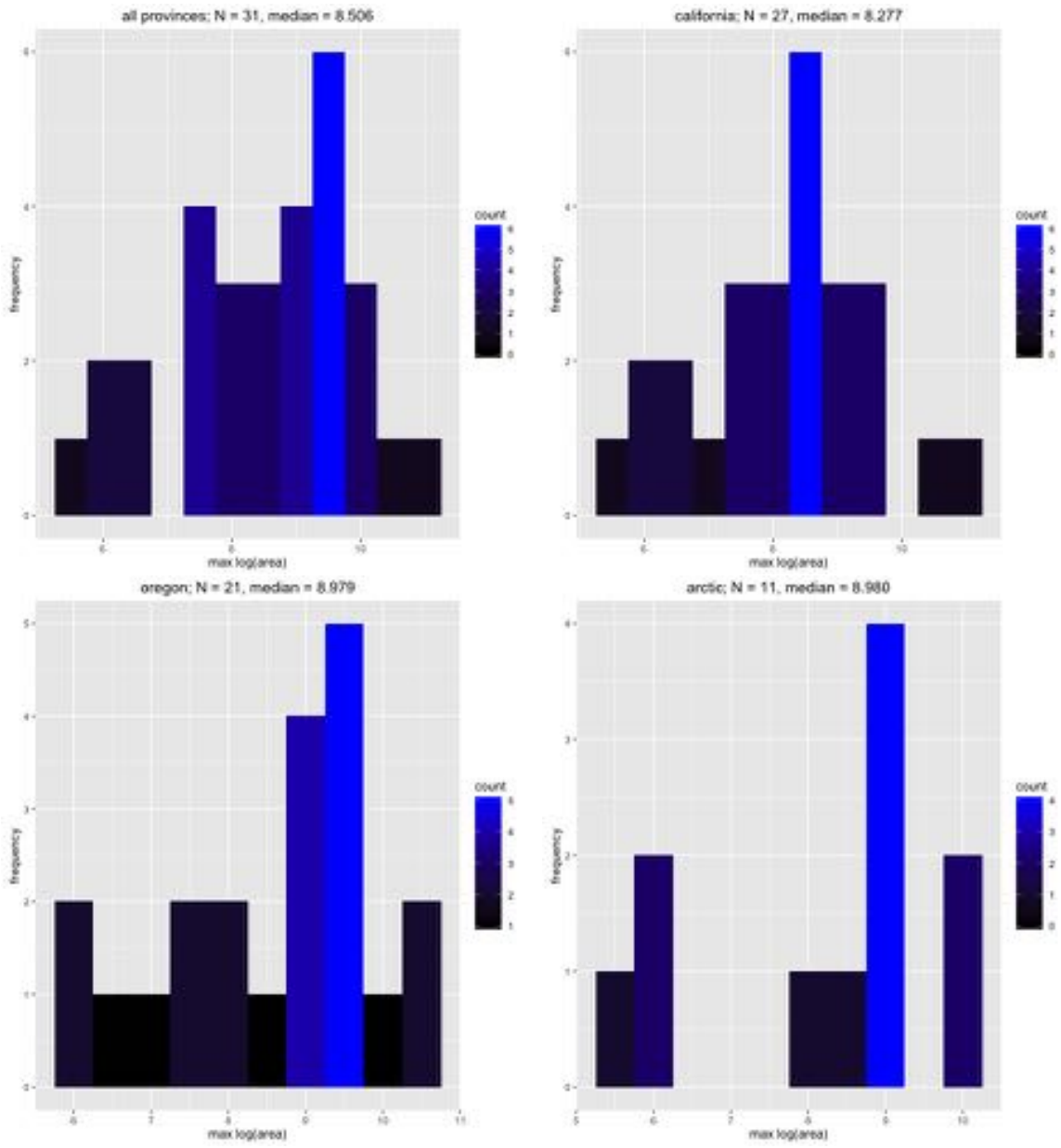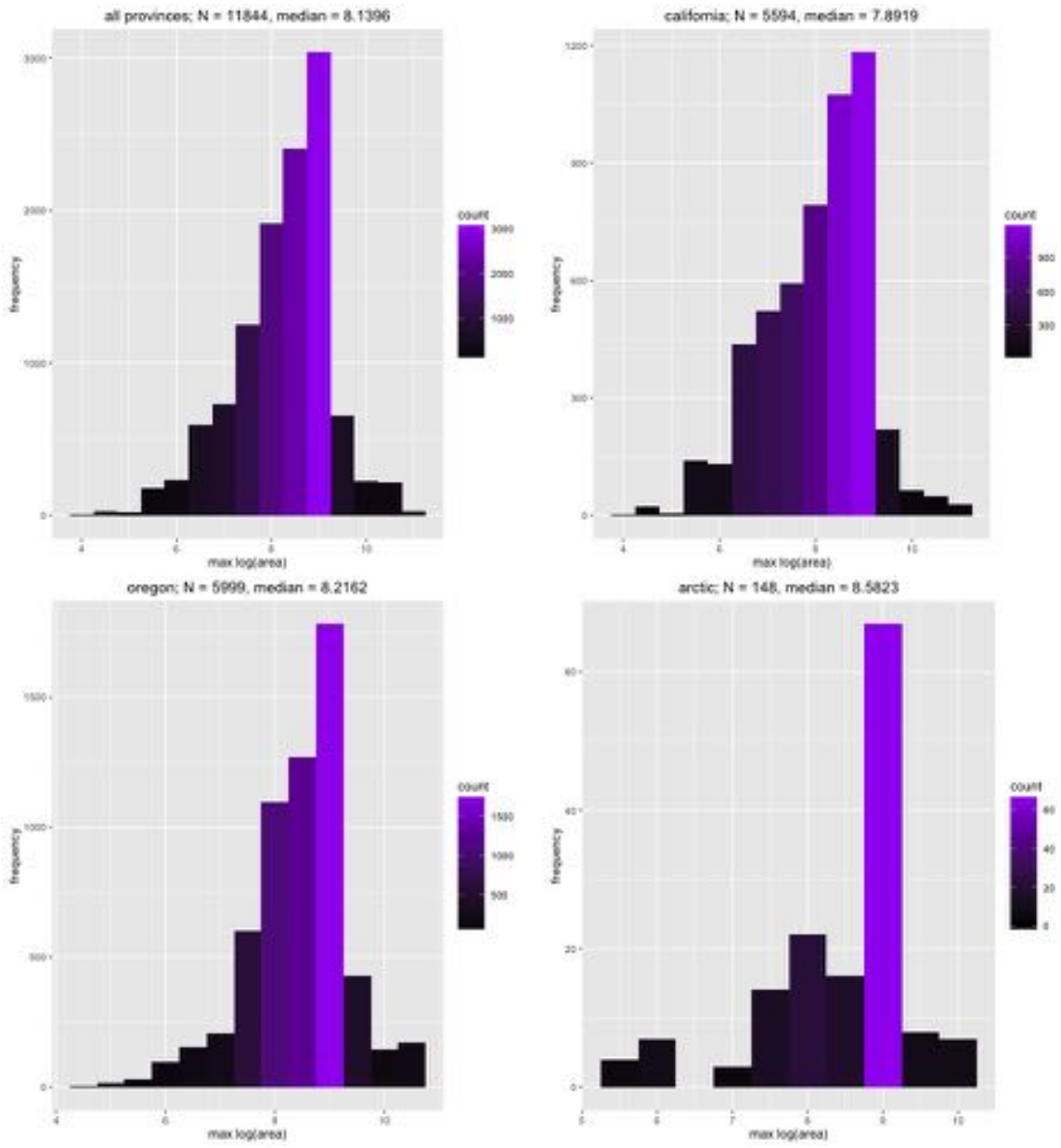
Figure 16: Size-frequency distributions generated using a provincial maximum for each species. N = the total number of individuals in each province, where max(logArea) is taken from provincial distributions and weighted by n.

species exemplars are used—has a large bearing on the trends observed in, and results obtained from, the data. For questions considering community structure, the robust approach is to collect data at an individual level, as results differ when using exemplar measurements. Increasing the number of exemplar measurements to reflect relative abundance is much better at capturing variation in trends than just using species' presence and absence to generate size distributions. However, even when these exemplar measurements are weighted by species abundance, they do a poor job at capturing overall trends. As such, not measuring individual variation changes the information available and ignores major patterns that would otherwise be apparent at a finer resolution.

Drivers of limpet community body size distributions

Environment does not drive community body size

While latitude does not explain variation in body size trends, traditional ecological theory would suggest that environment could be the best predictor of body size (Peters 1986). However, when sea surface temperature and Chlorophyll *a*, which strongly vary along the Eastern Pacific, are added into models, their explanatory power does not increase. None of the pairwise combinations of these environmental variables improves on a basic model, which uses latitude as the single predictor and explains very little variation in body size ($R^2 = 0.03$). It appears these abiotic models hit a goodness-of-fit plateau when expanded above a single predictor. This may be because the environmental covariates along the Eastern Pacific highly track latitude, and as such adding them to models that already contain a latitudinal predictor is redundant. However, given previous studies of size variation in response to environmental change (e.g. Atkinson 1997, Gardner et al. 2011), one would expect the environment to play a larger role in shaping size variation along this strong latitudinal gradient. A near-complete lack of influence may signal that, contrary to typical ecological belief, the environment does not play a strong role in shaping community structures through space, at least in Patellogastropoda.

It must be noted, however, that these findings come from a limited number of environmental variables, as this study only included information on SST and CHL along the transect. Our future work will incorporate further environmental factors, such as cloud cover,[15] which acts as

---

[15]See www.earthenv.org/cloud for the cloud cover dataset from Wilson and Jetz (2016).

a proxy for daily air temperature variation and humidity. While patellogastropods are marine, their position in the intertidal results in large amounts of exposure to terrestrial conditions, and as such inclusion of these terrestrial environmental variables may explain more variation in body size than the marine variables included in this study. Furthermore, this dataset will never contain information on the collection height of the individuals, and it is possible that position in the intertidal could be important in shaping size variability. As such, while our data shows that purely marine environmental variables do not explain body size trends, other, less traditional measures of environmental variability may be able to better explain variation.

Species composition is the primary predictor of body size

Models that incorporate species and faunal provinces as categorical variables, as well as the interaction between the two, highly predict body size in comparison to basic environmental models that lack biotic predictors. These biotic terms explain nearly 50% of the variation in size, and no pairwise additions of environmental covariates to biotic models improve their explanatory power. As such, it appears that it is not environment, but species composition, i.e. the species present and their organization in space, that is the primary determinant of body size distributions. It is important to note that not only do the species themselves explain a large amount of the variation in the data, as they account for the intraspecific variation that is so difficult to understand when looked at on a species-by-species basis, but that the provinces these species inhabit also aid in determining their sizes. This means that faunal communities, or how the species interact in space, are also significantly driving size trends. While this finding may seem abstract—that the groups of species surrounding an organism can affect its biomass production—it confirms Brown et al.'s (2004) statement that communities can interact to determine such individual-level processes.

Of course, at the moment it is uncertain whether interspecific interactions (e.g. competition and territorialism) are the true drivers of body size trends, or whether size is constrained on a individual level. In particular, our future work will focus on whether there are certain species combinations that lead to large- or small-bodied communities. If this work does not show that specific interactions aid in determining size structure, it may mean that assemblage size is determined more by the sizes that individuals can reach (which is itself constrained by the phylogenetic history of each species group). Because limpets are particularly prone to strong interspecific interactions (Fenberg 2011,

Lindberg 2015 pers. com.), species cohorts could be the underlying drivers of community structure as a predictor of size trends.

In sum, our data demonstrate that community structure predicts body size in Patellogastropoda, and that exemplar measurements do not reflect distributions obtained using individual-level data. As such, it follows that any studies attempting to investigate these trends must be conducted at an individual level. In addition, subsampling community-level data to be less detailed demonstrates further that removing individual variation from analyses of size can influence interpretations of trends. Following our analyses, it is clear that a proliferation of individual-level study of size trends is needed to further deconstruct the trends we find in the Eastern Pacific Patellogastropod group, as well as to determine whether these trends apply more broadly.

Consequences and further directions

If it holds across groups that community structure can drive body size variation, this may mean that any change in community structure can affect overall size distributions, and push average size in a given direction. If this is so, elevated rates of extinction, such as those associated with anthropogenic climate change (Waters 2016), could have larger-reaching biotic effects than expected, especially when these biotic shifts occur quickly (Benton 2009). Because body size is affected by and determines metabolism, development, and reproduction, along with nearly every other aspect of an organism's life history (Brown et al. 2004), any change in size results in a cascade of effects both for the organism itself as well as for the other organisms with which it interacts. It has been shown that organisms do experience size decreases in response to climate change (Sheridan and Bickford 2011). The move towards smaller body sizes is typically attributed to changing temperatures, as in many organisms temperature affects development and growth. This explanation, however, appears almost to be an "opposite-Bergmann" rule, which would state that an increase in temperature (which is closely correlated with latitude, the original Bermanian predictor) should result in a decrease in size. Perhaps, though, size decreases are not only caused by temperature, but also by changing community structure, which could be stronger driver on smaller timescales (Benton 2009). If the species present in a given space determine an individual's size, perhaps extinction could further exacerbate body size changes beyond the effects of a rapidly changing environment.

In order to understand this, studies of the effects of climate change on organismal size should use finer resolution data to account for individual variation, rather than focusing exclusively on environment as a primary predictor of size. Including faunal change in the equation may help to better predict short-term ecological responses to the pressures induced by anthropogenic climate change.

These questions will remain until they can be addressed further study, as they are beyond the scope of the current dataset. However, with our current data, we are able to investigate the underlying reason that community structure drives body size in Northeastern Pacific Patellogastropoda. In particular, these future studies will address whether a change in community structure (either via reshuffling or removal of species) would do the most to change size distributions, or whether this change is caused by the interactions among individuals. Perhaps in particularly competitive groups, such as the Patellogastropoda, an individual's body size *itself* can affect the body sizes other individuals obtain. Competitive individuals that lean large could potentially restrict the fitness, and thus the survival and reproduction, of smaller individuals, and in the process could constrain the range of body sizes seen in natural populations. In addition, we must gather more novel community data in order to determine whether biotic factors are the primary drivers of size on shorter-term scales for groups outside of the Patellogastropoda. to fully understand body size trends in ecologically variable groups, it must be first understood whether community structure is a *widespread* determinant of size, or whether it is most influential in highly competitive organisms. This can only be accomplished with individual-level data. Our macroscopic high-throughput imaging method provides the tools necessary to quickly compile these large-scale, individual-level datasets, and proves useful as a novel method for capturing community variation. Perhaps further study of individual-level trends will reveal that community structure plays a larger role in shaping individual size than was previously thought.

Acknowledgements

I am incredibly grateful to the people who have helped shape me both as a scientist and an individual. I would not have dared set foot into the world of Paleontology without the help of Pincelli Hull, who opened the doors to her lab and in doing so solidified my love for this field. I've found the scientific community to be welcoming and inspirational, due in no small part to support from my mentors, Leanne Elder, David Lindberg, Erin Saupe, and countless other people who've let me bother them in hallways and offices with endless questions. I've been blessed with more open doors than I can count: this study would not have happened had I not been hosted by Seth Finnegan and his lab, all of whom were willing to take a leap of faith in limpets. Kaylea Nelson and Allison Hsiang spent countless hours teaching me that, contrary to my luddite beliefs, computers are particularly useful. The Yale University Department of Geology and Geophysics provided me with the best network of supporters and friends I could have wished for during my time as an undergraduate. In addition, I cannot thank Greg Meyer enough for his unfailing support, which has immeasurably brightened my life—without him I would never have had the confidence to pursue a career in science. Lastly, and most importantly, I must thank Marta Segura and Robert Snelling for as their tireless work in raising and supporting me, as well as for their strong belief in the value of pursuing happiness. They are the sole reason I am able to receive a college education.

References

[1] Nasa goddard space flight center, ocean ecology laboratory, ocean biology processing group modis-aqua ocean color data. (2016).

[2] Ashton, K. G. Do amphibians follow Bergmann's rule? *Canadian Journal of Zoology* **80**, 708–716 (2002).

[3] Ashton, K. G., Tracy, M. C. & de Quieroz, A. Is Bergmann's rule vaid for mammals? *The American Naturalist* **156**, 390–415 (2000).

[4] Atkinson, D. & Sibly, R. M. Why are organisms usually bigger in colder environments? Making sense of a life history puzzle. *Advances in Ecological Research* **12**, 235–239 (1997).

[5] Babcock, L. E. & Robison, R. A. Taxonomy and paleobiology of some Middle Cambrian *Scenella* (Cnidaria) and Hyolithids (Mollusca) from western North America. *University of Kansas Paleontological Contributions* **121**, 1–22 (1988).

[6] Benton, M. J. The Red Queen and the Court Jester: species diversity and the role of biotic and abiotic factors through time. *Science* **323**, 728–732 (2009).

[7] Berke, S. K., Jablonski, D., Krug, A. Z., Roy, K. & Tomasovych, A. Beyond bergmann's rule: size-latitude relationships in marine bivalvia world-wide. *Global Ecology and Biogeography* **22**, 173–183 (2013).

[8] Blackburn, T. M., Gaston, K. J. & Loder, N. Geographic gradients in body size: a clarification of bergmann's rule. *Diversity and Distributions* **5**, 165–174 (1999).

[9] Blueweiss, L. *et al.*. Relationships between body size and some life history parameters. *Oecologia* **37**, 257–272 (1978).

[10] Bolker, B. M. *et al.*. Generalized linear mixed models: a practical guide for ecology and evolution. *Trends in Ecology and Evolution* **24**, 127–135 (2009).

[11] Bonner, J. T. Size and cycle: an essay on the structure of biology. *American Scientist* **53**, 488–494 (1965).

[12] Branch, G. M. The biology of limpets: physical factors, energy flow, and ecological interactions. *Oceanography and Marine Biology Annual Review* **19**, 235–380 (1981).

[13] Brown, J. H. *Macroecology*, (The University of Chicago Press1995).

[14] Brown, J. H., Gillooly, J. F., Allen, A. P., Savage, V. M. & West, G. B. Toward a metabolic theory of ecology. *Ecology* **85**, 1771–1789 (2004).

[15] Cooper, R. A. *et al.*. Completeness of the fossil record: estimating losses due to small body size. *Geology* **34**, 241–244 (2006).

[16] Daufresne, M., Lengfellner, K. & Sommer, U. Global warming benefits the small in aquatic ecosystems. *Proceedings of the National Academy of Sciences* **106**, 12788–12793 (2009).

[17] Fenberg, P. B. & Rivadeneira, M. M. Range limits and geographic patterns of abundance of the rocky intertidal owl limpet, *Lottia gigantea*. *Journal of Biogeography* **38**, 2286–2298 (2011).

[18] Gardner, J. L., Peters, A., Kearney, M. R., Joseph, L. & Heinsohn, R. Declining body size: a third universal response to warming? *Trends in Ecology and Evolution* **26**, 285–291 (2011).

[19] Grant, A. R. A revision of the California limpets of the genus *Acmaea* Eschscholtz (1933).

[20] Haven, S. B. Competition for food between the intertidal gastropods *Acmaea scabra* and *Acmaea Digitalis*. *Ecology* **54**, 143–151 (1973).

[21] Heim, N. A., Knope, M. L., Schaal, E. K., Wang, S. C. & Payne, J. L. Cope's rule in the evolution of marine animals. *Science* **347**, 867–870 (2015).

[22] Hull, P. M. *et al.*. Speeding up high-throughput, 3d-morphometrics with open code and data sharing (in prep).

[23] Jablonski, D. *Evolutionary Paleobiology*, chap. 10, 256–289, (University of Chicago Press1996).

[24] Kaspari, M. & Vargo, E. L. Colony size as a buffer against seasonality: Bergmann's rule in social insects. *The American Naturalist* **145**, 610–632 (1995).

[25] Klingenberg, C. P. & Spence, J. On the role of body size for life-history evolution. *Ecological Entomology* **22**, 55–68 (1997).

[26] LaBarbera, M. *Patterns and Processes in the History of Life*, 69–98, (Springer-Verlag Berlin1986).

[27] Lindberg, D. R. *The Light and Smith manual: intertidal invertebrates from central California to Oregon*, chap. Patellogastropoda, 753–761, (University of California Press2007).

[28] Lindberg, D. R. *The Patellogastropoda of the Northeastern Pacific* (in press).

[29] McLean, J. H. *West American prosobranch Gastropoda: Superfamilies Patellacea, Pleurotomariacea and Fissurellacea.*. Ph.D. thesis, Stanford University (1966).

[30] Meiri, S. Bergmann's rule-what's in a name? *Global Ecology and Biogeography* **20**, 203–207 (2011).

[31] Mora, C. & Robertson, D. R. Factors shaping the range-size frequency distribution of the endemic fish fauna of the tropical eastern pacific. *Journal of Biogeography* **32**, 277–286 (2005).

[32] Murphy, P. G. *Collisella austrodigitalis* sp. nov.: a sibling species of limpet (acmaeidae) discovered by electrophoresis. *Biology Bulletin* **155**, 193–206 (1978).

[33] Nakagawa, S. & Schielzeth, H. A general and simple method for obtaining r^2 for generalized linear mixed-effects models. *Methods in Ecology and Evolution* **4**, 133–142 (2013).

[34] Nakano, T. & Sasaki, T. Recent advances in molecular phylogeny, systematics, and evolution of patellogastropod limpets. *Journal of Molluscan Studies* **77**, 203–217 (2011).

[35] Orcott, C. R. *The West American Scientist: Molluscan World*, vol. 1 (1915).

[36] Partridge, L. & Coyne, J. Bergmann's rule in ectotherms: is it adaptive? *Evolution* **51**, 632–635 (1997).

[37] Payne, J. L., Heim, N. A., Knope, M. L. & McClain, C. R. Metabolic dominance of bivalves predates brachiopod diversity decline by more than 150 million years. *Proceedings of the Royal Society B* **281**, 1–8 (2014).

[38] Peters, R. H. *The Ecological Implications of Body Size*, (Cambridge University Press1986).

[39] Polly, P. D. *et al.*. History matters: ecometric and integrative climate change biology. *Proceedings of the Royal Society B* **278**, 131–1140 (2011).

[40] Ponder, W. F., Parkhaev, P. Y. & Beechey, D. L. A remarkable similarity in scaly shell structure in early cambrian univalved limpets (monoplacophora; maikhanellidae) and a recent fissurelid limpet (gastropoda: Vetigastropoda) with a review of maikhanellidae. *Molluscan Research* **27**, 153–163 (2007).

[41] Roy, K., Jablonski, D. & Martien, K. K. Invariant size-frequency distributions along a latitudinal gradient in marine bivalves. *PNAS* **97**, 13150–13155 (2000).

[42] Roy, K., Jablonski, D. & Valentine, J. W. Climate change, species range limits and body size in marine bivalves. *Ecology Letters* **4**, 366–370 (2001).

[43] Roy, K., Jablonski, D. & Valentine, J. W. Body size and invasion success in marine bivalves. *Ecology Letters* **5**, 163–167 (2002).

[44] Roy, K. & Martien, K. K. Latitudinal distribution of body size in north-eastern Pacific marine bivalves. *Journal of Biogeography* **28**, 485–493 (2001).

[45] Sheridan, J. A. & Bickford, D. Shrinking body size as an ecological response to climate change. *Nature Climate Change* **1**, 401–406 (2011).

[46] Simison, W. B. & Lindberg, D. R. On the identity of *Lottia strigatella* (carpenter, 1864) (patellogastropoda: Lottiidae). *The Veliger* **46**, 1–19 (2003).

[47] Sommer, U., Peter, K. H., Genitsaris, S. & Moustaka-Gouni, M. Do marine phytoplankton follow Bergmann's rule *sensu lato*? *Biological Reviews* (2016).

[48] Stimson, J. The role of the territory in the ecology of the intertidal limpet *Lottia gigantea* (gray). *Ecology* **54**, 1020–1030 (1973).

[49] Thomas, A. C., Srub, P. T., Weatherbee, R. A. & James, C. Satellite views of Pacific chlorophyll variability: Comparisons to physical variability, local versus nonlocal influences and links to climate indices. *Deep Sea Research II: Topical Studies in Oceanography* **77**, 99–116 (2012).

[50] Vinarski, M. V. On the applicability of bermann's rule to ectotherms: the state of the art. *Biology Bulletin Reviews* **4**, 232–242 (2014).

[51] Waters, C. N. *et al.*. The Anthropocene is fundamentally and stratigraphically distinct from the Holocene. *Science* **351** (2016).

[52] Wilson, A. & Jetz, W. Remotely sensed high-resolution global cloud dynamics for predicting ecosystem and biodiversity distributions. *PLoS Biology* **14**, e1002415 (2016).

[53] Xu, R. Measuring explained variation in linear mixed effects models. *Statistics in Medicine* **22**, 3527–2541 (2003).

Appendix

A brief introduction to Patellogastropoda

The majority of limpets occur in the rocky intertidal—a zone subject to immense change, as its daily variations in tidal level and high-impact shorebreak cause organisms living on the edge of the ocean to experience a high risk of dessication and physical stress as a result of constant wave action and large temperature fluctuations during tidal periods. Though they are not alone in their occupation of the shoreline, patellogastropods have evolved to be one of the species most tolerant of constant exposure to air and wave forces. They are able to occupy all three distinct areas in the intertidal: the upper intertidal, which is rocky and most dramatically exposed to air; the middle intertidal, where substrates are obscured by mussels, barnacles, and algae; and the low intertidal to subtidal, where substrate is mainly composed of kelps, fleshy seaweeds, and seagrasses.

Their evolutionary strategy for survival in these disparate environments—i.e. an uncoiled shell with a large aperture and a conical, low profile—is so successful that it has been copied by a number of other groups, all of which have taken on limpet morphology to such an extent as to be morphologically identical to the Patellogastropoda, the true limpets (*Reference needed*). Though a number of different groups have converged on the limpet body plan, these groups—including Fissurellidae, the keyhole limpets—these diverged much later than the Patellogastropoda. Until the advent of molecular phylogeny, the differences between and among these groups were nearly indiscernible; early taxonomists characterized limpets by their uncoiled shells and the presence of radula, but ignored minute morphological differences, and lacked the tools to understand the molecular relationships between limpet groups. In recent years, limpet taxonomy has been revised numerous times in an attempt to more accurately reflect new advances in gastropod evolutionary relationships.

Patellogastropod biology and taxonomy

Patellogastropods lie within the larger Gastropoda, a group which originated during the Cambrian and remained relatively stable in diversity until a Mesozoic increase and Tertiary explosion (Boardman et al. 1987, Heim et al. 2015). Gastropods are the most diverse and abundant mollusks, as they occur in marine, freshwater, and terrestrial environments. Most are mobile, benthic organisms with external shells; while these are typically coiled into a corkscrew helix, some have secondarily uncoiled their shells. Patellogastropoda (formerly known as Archaeogastropoda) is included in this latter group. The patellogastropod shell is conical, with a wide aperture and an apex that varies in position from central to anterior. Though the protoconch—the initial shell developed by the larval form—can sometimes attain coiling, it never develops a full whorl, and the adult form is wholly uncoiled (Lindberg 1984). Patellogastropods are characterized by torsion, a process by which the posterior mantle cavity and anus are rotated laterally and anteriorly in a counterclockwise direction such that they lie directly above the head. However, some show evidence of detorsion, which can

lead to varying degrees of bilateral symmetry.

Gross limpet morphology has remained unchanged since at least the Lower Cambrian, if not earlier (Babcock and Robison 1988, Ponder et al. 2007), so much so that most conical, univalved gastropods are defined as having a limpet-morphology. As such, gastropods that are considered to be "limpets" are not necessarily phylogenetic relatives of true limpets (patellogastropods). Within these true limpets, overt morphological characteristics are highly similar. Difficulties in distinguishing between species has resulted in a confusing taxonomic history, such that revisions to the patellogastropod phylogenetic tree have occurred a number of times throughout the late twentieth and early twenty-first centuries. While body characteristics, and in particular, radular characteristics, are useful for reliable, species-level identification, shell patterns and structure prove much more cryptic. Before the molecular age, patellogastropod taxonomists were faced with the daunting task of categorizing a group whose shell morphologies converge with habitat (such that species from similar habitats have similar shell morphologies), and whose intraspecific variation is so high that many species of patellogastropods have wildly different shell forms (e.g. the iconic *Lottia pelta*; Lindberg 1984). These variable forms are so distinct from one another that they can be confused with other species that occur in the same habitat (e.g. *L. digitalis* and *L. pelta* or *L. scabra*, and, prior to 1930, *L. persona*—see Lindberg 1984). In addition, within some species shells from either extreme of its distribution are often not recognized as conspecific (e.g. *L. paradigitalis*; Lindberg 1984).

While the advent of molecular phylogenetics, patellogastropod relationships became somewhat less difficult to decipher (e.g. Murphy 1978), and prompted massive revisions to the known phylogeny (achieved mainly by the malacologist and phylogeneticist D. R. Lindberg). While before the Eastern Pacific Patellogastropoda (formerly known as Docoglossa) were considered to comprise a single family (Acmaeidae), they now are split into seven: Lottiidae, Acmaeidae, Pectinodotidae, Lepetidae, Nacellidae, Patellidae, and Eoacmaeidae (Nakano and Sasaki 2011). Given the usefulness of shell morphology for identification (particularly for paleontologists), identifying characteristics for molecular groupings have also been updated. For this study, only those families that are present in the Northeastern Pacific (and, in particular, in the shallow subtidal and intertidal) are included. These updated groupings are as follows:

Acmaeidae

The majority of Acmaeids are found in deepwater environments of the northeastern Pacific. Most are associated with unique habitats such as sunken, waterlogged wood and oxygen-minimum zones; only two species—*Acmaea funiculata* and *Acmaea mitra*—are found in shallow subtidal areas near the coast (Lindberg 2007). Their ranges and brief descriptions can be found below.

Lottiidae

Lottiids are broadly distributed along the Pacific Rim, and are composed of several subclades; as such, this family includes a majority of Eastern Pacific patellogastropod species. Lottiidae includes all species (excluding the two Acmaeids) found along the Californian and Oregonian provinces. Many of these groups meet and transition in central California; in some locations as many as 16 species of both lottids and acmaeids can coexist (Lindberg 2007). Their ranges and descriptions can be found below.

- **_Acmaea atrata_**: ranges from Margarita Bay to Cabo San Lucas, Baja, Mexico (22.9°N) (Orcutt 1915). Shells have thick radial ribs which may be interspaced with smaller riblets. Often light in color, with darker inter-rib coloration. _A. atrata_ body stains are light, but cover a large portion of the shell interior.

- **_Acmaea funiculata_**: ranges from Shumagin Islands, Alaska (55°N) to Bahia Magdalena (24.5°N) and La Paz, Baja California, Mexico (24°N) (McLean 1996). Its shell is distinct in that it is almost entirely white (or sometimes white with irregular brown radial markings), and commonly encrusted in coralline algae (Lindberg 2007). _Synonymies: Acmaea mitra var. funiculata, Scurria mitra var. funiculata, Acmaea funiculata, Acmaea funiculata._

- **_Acmaea mitra_**: ranges from the Aleutian Islands, Alaska (52°N) to southern Baja California ($\sim$ 23°N) (Grant 1933). This species is typically found on rocky reefs covered in coralline algae which remain subtidal even at negative tides, and is typically solitary (Grant 1933). Its shell is white, oval, and lacks markings and ribbing (Lindberg 2007). _Synonymies: Acmaea mitra, Scurria mitra, Tectura mitra._

- **_Lottia asmi_**: ranges from southern Alaska ($\sim$ 58°N) to Isla Socorro, Baja California ($\sim$ 18.8°N). _L. asmi_ lives in the low- to mid-intertidal, often on _Chlorostoma_ spp., though some can be found on _Mytilus_ spp. and rocks. _Chlorostoma_-dwellers are laterally compressed with a high profile, while those that live on _Mytilus_ are flatter; the rock variety is similarly laterally compressed (Lindberg 2007). The rock-dwellers are lighter in coloration from the others; instead of being dark, they are grey-brown with occasional white tessellations (Lindberg 2007). _Synonymies: Patella (Acmaea) asmi, Nacelle asmi, Acmaea pelta var. asmi, Acmaea asmi, Collisella asmi._

- **_Lottia concreta_**: unknown.

- **_Lottia dalliana_**: ranges in the dataset from Tres Marias, Baja California, Mexico (25.9°N) to Gaviota Beach, California (34.8°N). _L. dalliana_ is flat, elongate, and dark brown in color with fine riblets and light-colored dots that run parallel to the length of the shell. Body stain is light and concentrated apically. The apex of the shell is posterior, and the part of the shell immediately surrounding the apex can be raised in relation to the shell's overall flatter profile.

- **_"Lottia" depicta_**: along with _"Lottia" palacea_, is more closely related to lotiiids found in the New World tropics than to the other Eastern Pacific lottiids. _Lottia depicta_ ranges from Mugu Lagoon, California (34°N) to Cabo San Lucas, Baja California, Mexico (22.9°N) (McLean 1966). The northern range of _L. depicta_ is often extended by El Niño events to Monterey Bay, California (38.6°N) (Lindberg 2007). _L. depicta_ is associated with the eelgrass _Zostera marina_, which occurs in estuaries and offshore. Estuarine specimens are elongate and laterally compressed, while offshore specimens are more ellipsoid given the wider blade with of _Zostera_ in these habitats (Lindberg 2007). Its shell color is typically light yellow, and can contain brown-red chevron markings and concentric growth lines (Lindberg 2007). _Synonymies: Patelloida depicta, Nacella depicta, Acmaea (Collisella) depicta, Collisella (Notoacmaea) depicta, Tectura depicta._

- **_Lottia digitalis_**: ranges from Attu Island, Aleutian Islands, Alaska (52.9°N) to Cabo San Lucas, Baja California (22.9°N) (Lindberg 2007). This species is often infected by a marine fungus, _Pharcidia balani_, which causes shell erosion and can severely alter shell coloration and

sculpture. The shell is highly ribbed (resulting in the species' common name, 'finger limpet'); these ribs are rounded and strongest on the posterior slope of the shell, so much so that they may be absent at the anterior end (Lindberg 2007). *Synonymies: Acmaea digitalis, Acmaea digitalis, Patella (Acmaea) digitalis, Acmaea (Collisella) digitalis, Tectura digitalis, Acmaea persona var. digitalis, Collisella digitalis, Lottia digitalis.*

- **Lottia discus**: may be a curatorial misspelling of *Lottia discors*, a Panamic species ranging from Cabo San Lucas, Baja California, Mexico (22.9°N) to Panama.

- **Lottia fenestrata**: ranges from the Shumagin Islands in Alaska (55°N, 161°W) to Punta Pequeña, Baja California, Mexico (26.14°N) (McLean 1966). There are distinct differences in ecology in the northern population, which occupies the coast from northern Alaska to Point Conception, California, and the southern population, which extends from Point Conception to southern Baja California. The northern population is found in the lower and middle intertidal zones on the sides of rocks and boulders surrounded by loose sand, while the southern population is found on rubble reef habitats, typically alongside eel grass *Phyllospadix spp.* (McLean 1966). As a result, northern *L. fenestrata* often look "sandblasted" or scoured, as their typical external markings are worn smooth by the movement of sand over their shells. Often the apex will erode first, exposing the shell's brown underlayers, but in more advanced specimens, the majority of the shell is polished and brown. *L. fenestrata* is the only west American species that occurs in brackish, hyposaline waters, and can withstand periodic freshwater conditions (McLean 1966). Its shell is compressed, thin, and broadly oval; the outer portion is typically tinted blue to blue-grey, with occasional riblets and small white tessellations that increase in size as they extend towards the outer margins of the shell. The interior of the shell is blue, and is often almost completely tinted a brownish hue. Its liver stain is dark and prominent. Given that the mantle of living specimens is also stained brown, and that its diet is high in trace metals given the typically barren substrate this species frequents, the coloration is likely due to high amounts of mantle secretion. *Synonymies: Patella fenestrata, Acmaea patina var. fenestrata, Acmaea fenestrata, Collisella (Notoacmaea) fenestrata, Tectura fenestrata.*

- **Lottia gigantea**: ranges from Monterey Bay, California (38.6°N) to Punta Eugenia, Baja California (27.8°N). The species' northern latitude has contracted by over 2 degrees since 1963, while the southern limit has remained stable (Fenberg and Rivadeneira 2011). This limpet is highly territorial, and this behavior is reflected in its shell morphology—its apex is pushed nearly to its anterior limit, transforming the shell into a miniature 'plow' which is used to push competitors off of the territory in question. Size plays a large part in the growth of *L. gigantea* individuals; smaller specimens are much more efficient grazers, but are often hindered by larger, less-efficient competitors—i.e. small limpets are kept small by large territory-holders (Stimson 1973). *Synonymies: Scurria (Lottia) gigantea, Patella kochi, Tecturella grandis.*

- **Lottia insessa**: ranges from Wrangell, Alaska (56.2°N) to Bahia Magdalena, Baja California, Mexico (24.5°N) (McLean 1966). This low-intertidal species is believed to live and feed exclusively on the holdfast of *Egregia menziesii* (feather boa kelp), and this close relationship is reflected in their shell color. Individuals vary in color from orange to very dark brown, and each individual's color may correspond with their latitude (Coston and Lindberg, unpublished). The apex can be rounded, and will often curve towards the shell's posterior. Body stains are very dark, and cover the majority of the shell's interior. *L. insessa* specimens are small, ranging anywhere from 1 to 20 mm in length. *Synonymies: Patella insessa, Nacelle*

insessa, Acmaea insessa, Collisella (Notoacmaea) insessa.

- **Lottia instabilis**: ranges from Amchitka, Aleutian Islands, Alaska (51.75°N) to San Diego, California (32°N). *L. instabilis* presents in kelp form, solid form, and tesselate form. The bottom edge of the kelp form's shell is typically rounded, such that when made to stand upright it will rest on one end or another of the major axis (like a rocking horse), and the shell is typically elongate. The apex of the kelp form shell is often weathered, and as such is lighter in color. The solid form shell is more typically conical; the bottom edge is flat, and the shell can be colored from off-white to brown. The tesselate form has spotted (tesselate) markings across the top of the shell. All forms have thin, straight radial riblets and light body stains. *Synonymies: Patella instabilis, Nacella instabilis, Acmaea instabilis, Collisella instabilis.*

- **Lottia limatula**: ranges from Newport, Oregon (44°N) to Isla Socorro, Revillagigedo Islands, Mexico (19°N) (McLean 1966). Southern Californian specimens have two wide posterior rays of tessellations, while specimens from estuarine habitats as well as those that live in the high intertidal have tall, elevated shells (Lindberg 2007). These limpets are distinguishable by their small riblets, which have an overlapping, scaly texture. *Synonymies: Acmaea scabra var. limatula, Acmaea limatula, Acmaea (Collisella) limatula morchii, Collisella limatula.*

- **Lottia mesoleuca**: ranges from Ecuador to San Felipe, Baja California, Mexico (31.03°N). The shell is highly distinguishable by its bright blue underside. It has small radial riblets and is typically light brown in color, with white tessellate markings that loosely follow these radial riblets. The body stain of *L. mesoleuca* is dark green to brown when present.

- **Lottia ochracea**: is the solid and tessellate forms *L. instabilis*.

- **"Lottia" paleacea**: ranges from Vancouver Island, British Columbia, Canada (49°N) to Camalu, Baja California, Mexico (30°N) (McLean 1966). Also known as the surfgrass limpet as it is found only on *Phyllospadix* spp. Its shell is elongate, thin, and light in color, though is sometimes colored with brown streaks. Some *L. paleacea* shells may have small parallel riblets that extend anteriorly from the posterior apex. *Synonymies: Acmaea paleacea, Nacella paleacea, Collisella (Notoacmaea) paleacea, Tectura paleacea.*

- **Lottia paradigitalis**: ranges from Attu Island, Aleutian Islands, Alaska (53°N) to Point Conception, California (34.25°N) (Simison and Lindberg 2003). This high to mid-intertidal limpet is highly morphologically similar to *L. digitalis*, though it typically lacks apical weathering and is instead distinguishable by tessellate patterns near the rim of the shell as well as by a chevron pattern surrounding the apex. This species is often found on vertical surfaces and the shells of other mollusks (in particular, turban snails and *Mytilus* spp.; Lindberg 2007). *Synonymies: Acmaea pelta x digitalis, Acmaea (Collisella) paradigitalis, Acmaea persona strigatella, Acmaea patina var. strigillata, Collisella striggtella, Collisella borealis, Acmaea (Collisella) radiata.*

- **Lottia patina**: is a synonymy of *L. scutum*.

- **Lottia pelta**: ranges from Hokkaido, Japan (41°N, 136°E) to the Aleutian Islands, Alaska at the northernmost end of its range, and south to Punta Rompiente, Baja California, Mexico (27.4°N) (Lindberg 2007). This species is phenotypically plastic, and undergoes large morphological changes as a result of its habitat (changes which may be driven by diet). The rock form of *L. pelta* is crenulate, as its shell contains large and wide ribs, and its growth lines are

coarsely visible. It is light in color, though its apex weathers to a dark, smooth finish. The *Mytilus* form of *L. pelta* (which is aptly named, as it lives on *Mytilus* spp.) is smooth and dark, with a high apex. The kelp form is flatter than its two counterparts, has visible growth lines, and light radial riblets. These forms can often also have white spots or faint tessellations coloring their shells. All forms are identifiable by their very dark body stains. *Synonymies: Acmaea pelta, Patella (Acmaea) pelta, Acmaea cassis var. pelta, Collisella pelta, Acmaea cassis, Patella cassis, Tectura cassis, Patella fimbriata, Patella (Acmaea) aeruginosa, Patella (Acmaea) pileolus, Patella cinis, Patella nuttalliana, Patella leucophaea, Patella monticola, Acmaea cassis monticola.*

- **Lottia persona**: ranges from Shumagin Islands (55°N) to Morro Bay, California (35.5°N). A nocturnal species that is and abundant in high and middle intertidal zones, where it inhabits caves and cracks during the day. *L. persona* is commonly known as the mask limpet due to its large white markings, which are concentrated into symmetrical, lateral rays (Lindberg 2007). Has distinct northern and southern forms, where northern specimens' marking rays are much shorter. Anterior markings are translucent and allow the living limpet to assess ambient light conditions (Lindberg 2007). *Synonymies: Acmaea persona, Patella (Acmaea) persona, Tectura persona, Collisella (Notoacmaea) persona, Acmaea ancylus, Acmaea radiata.*

- **Lottia rosacea**: ranges from Ketchikan, Alaska (55°N) to Isla de Guadalupe, Baja California, Mexico (29°) (McLean 1966). This limpet is pink in color, often with white streaks and dots ranging in color from white to yellow-brown. Its shell is often smooth; if ribbed, these are small, fine, and radial. Body stains are faint or nonexistent. *Synonymies: Acmaea pileolus var. rosacea, Acmaea rosacea.*

- **Lottia scabra**: ranges from Cape Arago, Oregon (43.2°N) to Cabo San Lucas, Baja California, Mexico (23°N) and Isla Socorro, Revillagigedo Islands, Mexico (19°N) (McLean 1966). *L. scabra* is a middle intertidal limpet that occurs on horizontal surfaces (Lindberg 2007). This limpet is highly crenulate, and has large radial ribs interspaced with many smaller, pronounced ribs, contributing to making the limpet's margin look rugged and rugose. The shells of *L. scabra* are light in color, sometimes with darker apical spots. When dropped, these shells create a tinny sound that is at a higher frequency than other limpet shells, indicating a difference in mineral arrangement. This limpet creates distinct home scars, with which they are very highly associated. They are often found on the shells of larger *L. gigantea* specimens (which are highly territorial), though their choice of substrate does not diminish the intensity of their scar formation. *Synonymies: Patella scabra, Acmaea scabra, Collisella scabra, Patella spectrum, Acmaea spectrum.*

- **Lottia scutum**: ranges from Akkeshi Bay, Hokkaido, Japan (43°N, 145°E) to the Kurile Islands, Aleutian Islands, Alaska in the northernmost end of its range, and south to San Pedro, California (33.5°N) (McLean 1966). *L. scutum* is a middle to low intertidal limpet with strong, radially tessellate patterns and a dark body stain. These shells are thick, and apex position changes with size (Lindberg 2007). *Synonymies: Acmaea scutum, Collisella (Notoacmaea) scutum, Tectura scutum, Acmaea patina, Patella patina, Tectura patina, Lottia pintadina, Patella (Acmaea) ancyloides, Patella (Acmaea) pintadina, Patella verriculata, Patella cumingii, Acmaea testudinalis, Acmaea emydia, Collisella emydia, Notoacmaea emydia.*

- **Lottia stanfordiana**: Found exclusively in the dataset near Puertecitos, Baja California (30°N). The light blue underside of the *L. stanfordiana* shell has growth lines which are

clearly visible. The top of the shell has fine radial riblets and small white dots which extend radially from the apex, and is colored in distinct rings which can range from dark brown to light yellow.

- **Lottia strigatella:** is a synonymy of *L. paradigitalis*.

- **Lottia testudinalis:** a circumarctic species that ranges from Point Barrow, Alaska (71°N) to Attu Island, Aleutian Islands, Alaska (53°N). The shell of *L. testudinalis* is smooth and light in color with dark brown, radial or tessellate streaks. *L. testudinalis* has a dark brown body stain. *Synonymies: Patella testudinalis, Notoacmaea testudinalis, Tectura testudinalis, Patella tessulata, Patella clealandi, Patella amoena, Patella clypeus, Acmaea fergusoni.*

- **Lottia triangularis:** ranges from Port Dick, Alaska (59.16°N) to Santa Barbara, California (34.5°N) (McLean 1966). Its shell is white, ellipsoid, and laterally compressed, often containing a few small brown rays or a small brown apical spot (Lindberg 2007).

- **Lottia turveri:** ranges from the Sea of Cortéz, Mexico to San Felipe, Baja California, Mexico (31.02°N). This limpet has a highly crenulate shell, with large radial ribs and a shell margin similar to that of *L. scabra*, but lacking in smaller riblets. *L. turveri* is light in color, sometimes with darker tessellations near the margins of the shell, and often weathered or encrusted with algae.

Importance of modern-paleo comparisons

Fossil-modern calibrations are imperative for the advancement of paleontological knowledge—for, as one would expect, it is nearly impossible to decipher an ancient system without first understanding its modern analog. While some systems have been adequately deconstructed, far more remain mysterious, so much so that we know little about a vast majority of eco-evolutionary history. Perhaps one of the most pressing gaps in our knowledge, especially given the current state of rapid climate change, is that of how changing conditions affect growth, morphology, and abundance, especially for those organisms that live in highly variable environments. While the causal mechanisms that underly the changes brought about by environmental fluctuation will take much more investigation to fully deconstruct, observing their affect on ecological communities is much less difficult.